EMPIRICAL APPROACH FOR RATE SELECTION IN MIMO OFDM

Anil Madhava Hebbar

Thesis submitted to the Faculty of the

Virginia Polytechnic Institute and State University

in partial fulfillment of the requirements for the degree of

MASTER OF SCIENCE

In

Electrical and Computer Engineering

Dr. Jeffrey H. Reed (Chairman)

Dr. Brain D. Woerner (Committee Member)

Dr. Annamalai Annamalai (Committee Member)

Blacksburg, Virginia

17th December 2004

Keywords: OFDM, MIMO, SVD, Frequency fading, 802.11n TGn Sync

EMPIRICAL APPROACH FOR RATE SELECTION IN MIMO OFDM

ANIL M. HEBBAR

ABSTRACT

Orthogonal Frequency Division Multiplexing (OFDM) is fast gaining ground as a preferred modulation technique for short range wireless data application such as 802.11a/g, 802.15.3a and 802.16. Recently, use of multiple transmit and receive antenna for improving spectral efficiency in a wireless system has received much interest. IEEE 802.11 has set up the Work Group 802.11n to develop a standard for enhanced rate 802.11 based on OFDM using Multi Input/Multiple Output (MIMO) techniques. The most dominant proposal is the use of singular value decomposition based MIMO methods to achieve the high data rate.

The selection of modulation and coding rates plays a significant role in the overall throughput of the system, more so in cases where the traffic between the transmitter and the receiver consists of short bursts and the user location is not fixed. The performance of a given modulation and coding technique depends on the channel condition. Closed form or bounding solutions exists for various modulation and coding techniques. But these techniques are not suitable for real time application where the channel is dynamic.

The approach taken in this thesis is to decouple frequency selective MIMO OFDM channel into orthogonal spatial and frequency domains channels using Fast Fourier Transforms and Singular Value Decomposition. The channels can be viewed as parallel flat fading channels for which the expected BER rate can be computed. A SNR-BER table is used to efficiently compute the performance efficiently. An effective SNR is computed using the table and compared with rate threshold to select a suitable rate. Improvements of 15 dB and above are shown the link budget while using a four transmit four receive MIMO system.

Proposed 802.11n TGn Sync physical layer standard is used to evaluate the performance. The performance in case of one of the systems being a legacy 802.11a/g nodes is also looked into. Gains up to 7 dB are shown in the link budget.

Acknowledgements

I would like to thank Dr. Reed for allowing me the opportunity to work at MPRG, being the chairperson of my thesis committee and offering useful pointers during the course of my research.

I would like to express my gratitude to committee members Dr. Woerner and Dr. Annamalai for being in the committee and offering valuable advices and inputs at various stages of my research. Thanks also to Dr. Buehrer for his help in deciphering the physical layer OFDM standards.

I wish to express my appreciation to MPRG post-docs Dr. Max Robert, Dr. James Hicks, Dr. Raqibul Mostafa and members of MPRG staff for their support.

Thanks in no particular order to MPRG students Ramesh Palat, Swaroop Venketsh, Jihad Ibrahim, James Neel and Chris Anderson for their help and advice.

I wish to put on record my appreciation for the excellent reference letters and support from Dr. Paul Petrus, Dr. Doug Dhalby and Todd Larsen and rest of the folks at Arraycomm.

My work was supported by Mercury Computer Systems and some of my algorithms were tested on hardware provided by them and Spectrum Signal Processing for whom I own my gratitude. I own my thanks to Office of Naval Research, who funded my work at MPRG.

I wish to thank and dedicate this thesis to my wife Jyoti and my family for their support of my work.

TABLE OF CONTENTS

LIST OF FIGURES

LIST OF TABLES

1 Introduction

Wireless communication for using Wireless Local Area Networks (WLANs) is now being considered as a viable solution for providing ubiquitous network connectivity to a wide array of military, industrial, consumer electronics users. The applications range from ad-hoc emergency networks, tactical situation awareness network for battlefield applications, to more day to day applications such surfing the web at the mall, audio or video downloads and internet gaming. Two requirements that are of increasing importance are security for WLAN applications and higher data rates to support applications using the internet. This thesis deals with improving data rate in WLAN systems.

LANs were initially used to support low data rate text messages and hence the initial LAN was slow by today's standards. Current internet applications function well with average speeds of 300 kbps. Future applications such as internet gaming and TV on demand would require much higher bandwidth (in the order of 10s of Mbps) and lower latency. Therefore, significant R&D efforts have been directed towards faster data rate LANs and WLANs. Some of the promising technologies being explored in the WLAN domain are the UWB pico-cells, 802.11 series of WLAN and WiMax. With the exception of 802.11a/b/g, other WLAN applications are in the development or trial stage and yet to be commercialized.

802.11 use two different sets of over the air interface to get the high data rate. 802.11b employs Direct Sequence Spread Spectrum (DSSS) and gives a maximum data rate of 11 Mbps. 802.11a, 802.11g and the proposed high throughput 802.11n use Orthogonal Frequency Division Multiplex (OFDM) in the physical layer.

IEEE 802.11a uses 20 MHz spectrum at 5 GHz and has data rates ranging from 6 Mbps to 54 Mbps. 802.11g has the same physical layer as 802.11a for the higher data rates but uses the 2.4 GHz spectrum.

IEEE 802.11n may use 20 MHz or an optional 40 MHz bandwidth at 2.4 GHz spectrum. The research done for this thesis assumes a 20 MHz bandwidth. Another feature of 802.11n is the use of Multiple Input Multiple Output (MIMO) systems. For MIMO systems, it has been shown by Gans and Foschini [9] that the capacity of a system could be made to

increase linearly with the number of antennas. The main focus of this research is to examine MIMO OFDM for application in 802.11n like physical layer and try to come up with a way to select the rate based on channel conditions. Important criteria to be kept in mind are speed and complexity constraints so that implementation is possible in real time systems. Also, since 802.11n has to be backward compatible with legacy 802.111/g system, it is imperative that the proposed scheme be usable in a mixed system environments. Scalability in terms of number of antennas is also a useful feature to have.

The Singular Value Decomposition (SVD) based MIMO technique has been proposed as a possible method to achieve the above objectives by the TGn group of IEEE.

This chapter deals with the area of focus of the thesis, analysis method, chapter description and literature related to this area.

1.1 Area of focus

The thesis investigates the performance of SVD MIMO techniques in 802.11 OFDM physical layer and approaches to improve throughput. Throughput depends on the modulation and coding employed. 802.11n proposals suggest using convolution, block or Low Density Parity Check (LDPC) codes for channel coding. For optimum rate selections, channel code performance in a given channel is crucial. While there exists some work on block and LDPC code performance on fading channels, there is not much literature dealing with convolution codes in fading channels. The thesis tries to bring out the problems encountered in finding an analytical solutions and suggests and alternate empirical solution for selection of rate when convolution codes are used.

1.2 Method of analysis

The thesis develops and uses equivalent frequency domain model to obtain the performance of the selected rate by simulation. A Single Input Single Output (SISO) frequency domain model is first built from the tap delay channel model in time domain. The model is then extended into the spatial domain using the SVD. Analytical Bit Error Rate (BER) performance for a given modulation class can also be obtained from this models and illustrated with an example using BPSK modulation.

1.3 Chapter description

In Chapter 2, the basic principles of OFDM are discussed and the relevant 802.11a/g OFDM physical characteristics are studied. Salient points of the proposed TGn Sync proposal are explained.

Chapter 3 looks into the 802.11 OFDM performance in Single Input Single Output (SISO) channel, using the IEEE TGn Channel Models [6]. The chapter introduces the concept of decomposition of frequency selective fading channel into parallel flat fading channels in the frequency domain. The frequency domain channel model is used to simulate the performance for different data rates. The concepts of effective SNR and effective SNR based rate selection are introduced.

Chapter 4 extends the concept of decoupling of frequency selective channel to spatial domain. The initial part of the chapter introduces Singular Value Decomposition (SVD) based approach to decouple flat fading MIMO channels into orthogonal spatial channels. The second part of the chapter combines the SVD based spatial decoupling with FFT based frequency domain decoupling and indicates ways of applying the threshold technique of rate selection to judge the channels.

Chapter 5 introduces two techniques that make use of the threshold method to select data rates. The simulations results are presented and compared. The backward compatibility with 802.11a/g single antenna systems is shown.

Chapter 6 concludes the thesis by discussing some of the expected problems and scope for further research.

Appendix 1 discuss the TGn channel model. The channel model is used to generate the SISO and MIMO channels used in the thesis.

Appendix 2 discuss the SVD. Some important properties and a possible method to implement the SVD are discussed.

1.4 Background and literature survey for the research:

The research started as a class project to study beam forming applications in 802.11a/g. The initial research and chapter 2 is based on the project and the subsequent conference paper.Subsequent sections are based on the 802.11a PHY [7] standard and 802.11n TGn Sync proposal [8]. The basic OFDM information was from the book on the subject [2]. The bit error rate for modulation and convolution coding and lot of the groundwork are from the books [1] and [3] on communication theory and coding. The linear algebra derivations are based on [4].

Channel modeling information was mostly derived from TGn channel models form IEEE TGn web site [6]. Additional insights were obtained from the paper by Forenza, Love and Dr. Heath [14].

One of the first analytical work done on MIMO channels is the paper by G.J. Foschini and M.J. Gans [9]. The paper extends the Shannon's channel capacity to MIMO channels.

The paper [15] and [16] and deals with the theoretical capacity of MIMO systems using OFDM.

The Vertical Bell Labs Layered Space-Time (V-BLAST) proposed by Bell labs [9] was one of the first schemes that used MIMO channel to send parallel symbols streams from the transmitter. The main disadvantage with this scheme is that the channel estimation needs to be good, which requires high SNR. Classical V-BLAST requires flat fading channel which leads to narrow band channel assumptions and use of multiple transmit and receive antennas (of the order of 10-16) in order to achieve high throughput rates. This makes it impracticable for portable WLAN applications.

S. Alamouti. [19] proposed the use of Space-Time Codes (STC). The problem with this technique is that there are no full rate codes when there are more then two transmit antennas. Also, like the V-BLAST techniques, the performance degrades when the channel in not flat fading,

Considerable research has been done in both the in V-BLAST and STC techniques to overcome problem of flat fading constraints by using OFDM. BLAST and OFDM are investigated in the paper [20]. [21] deals with implementation of STC in an OFDM system.

There have been some works on performance bounds for block or low density parity check (LDPC) codes in a fading environment ([17] and [18]). They provide bounds for performance in a fading channel. But similar bounds have not been determined for convolution code.

2 Fundamentals of OFDM, 802.11a/g and 802.11n

OFDM as a modulation technique was first proposed by Chang of Bell Labs in 1966 in a paper on the above topic. In 1971, Weinstein and Ebert proposed the use of FFT to implement the system practically. However, the advent of fast digital signal processors and FPGAs in the mid 1990's provided the real opportunity to effectively implement OFDM systems.

OFDM finds application in areas such as terrestrial Digital Audio Broadcast (DAB), Digital Video Broadcast (DVB), Digital Subscriber Lines (DSL) and Wireless network standards such as IEEE 802.11a/g/n and HiperLan/2 and the proposed IEEE 802.16. The main focus of this chapter is the overview of OFDM and it's use in 802.11a/g/n physical link layer.

This chapter provides an overview of OFDM technique. The 802.11a/g physical details such as frames, symbols and training sequence are discussed and nomenclature is explained. The proposed 802.11n TGn Sync proposal features relevant to the thesis are covered.

2.1 OFDM modulation technique

Consider a time domain sinusoidal signal of the form $e^{j\omega_c t}$, where $\omega_c = 2\pi f_c$. The frequency domain representation of this is an impulse at $\omega = \omega_c$. Now, this signal is sampled using a rectangular window of period *T* seconds, with N samples taken at intervals of *T*/N seconds. Assuming the frequency of interest is within the Nyquist interval, the resulting samples are given by

$$x(n) = \begin{cases} e^{j\omega_c n/N}, 0 < n < N-1 \\ 0, \ otherwise \end{cases}$$

In time domain, this is product of rectangular window of length N with sinusoid. The frequency domain representation would be the convolution of the Discreet Fourier Transform (DFT) of the two. The DFT of a rectangular function is a sinc function, whose

magnitude spectrum is given $\frac{\sin(\omega N/2)}{\sin(\omega/2)}$. This function has peak at ω = 0 and zeros at $\omega = \pm 2\pi k/N$, k is an integer in the range –N/2 to N/2, excluding k = 0.

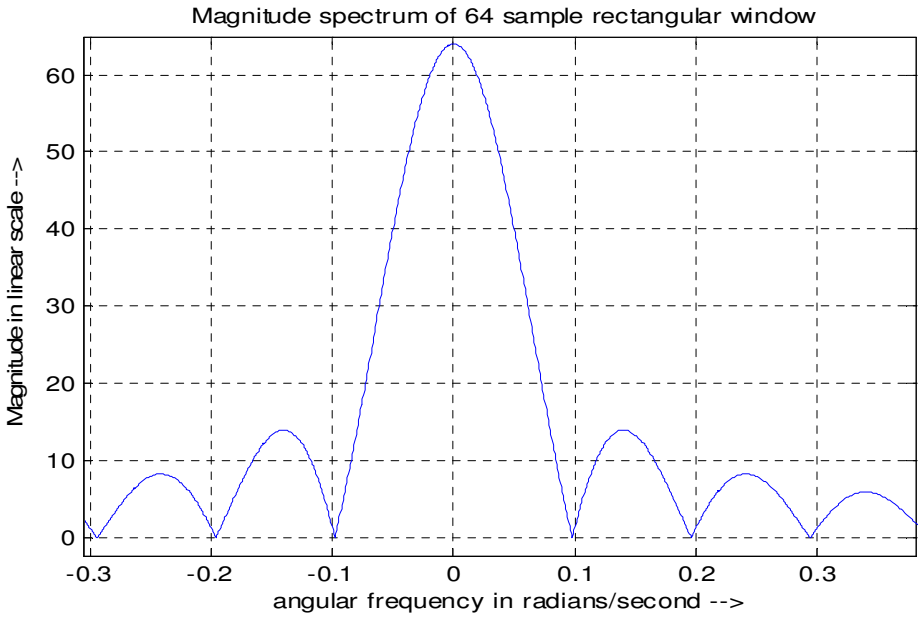

Figure 1: Magnitude spectrum of 64 sample rectangular window

Figure 1 shows the sinc function for a 64 sample rectangular window, with T = 1/64. The points have been interpolated to produce a continuous curve for purpose of display clarity. The zeros of the function are found at angular frequency $\omega = \pm\frac{2\pi}{64}, \pm\frac{4\pi}{64} \ldots .$

The result of the convolution with an impulse at $f = f_c$ is that the sinc function is shifted from peak at ω = 0 to peak at the angular frequency corresponding to $\omega = \omega_c$. The zeros occur at angular frequencies

$\omega = \omega_c \pm \frac{2\pi}{64}, \omega_c \pm \frac{4\pi}{64}$, where $\omega_c = 2\pi f_c$

Figure 2 shows the plot for a frequency $f_c = 16/T$ sampled with N = 64.

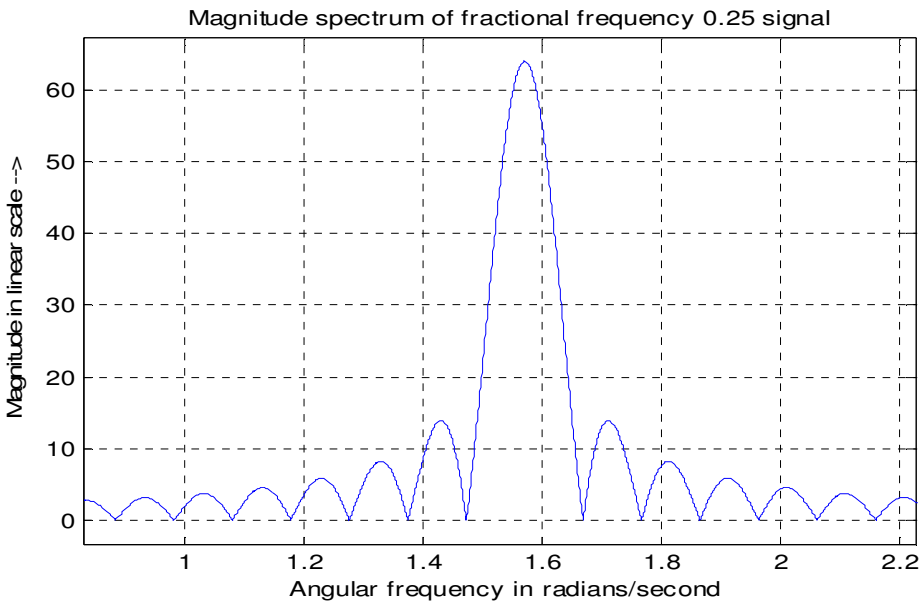

Figure 2: Frequency plot for 0.25 fractional frequency sinusoid sampled using 64 sample rectangular window

Here, it is seen that the zeros occur at $\omega = 2\pi\left(0.25 \pm \frac{1}{64}, 0.25 \pm \frac{2}{64} .....\right)$

This indicates that if the frequency components of a signal are separated by intervals of 1/N, they will not interfere with each other. A plot of such a signal is shown in Figure 3.

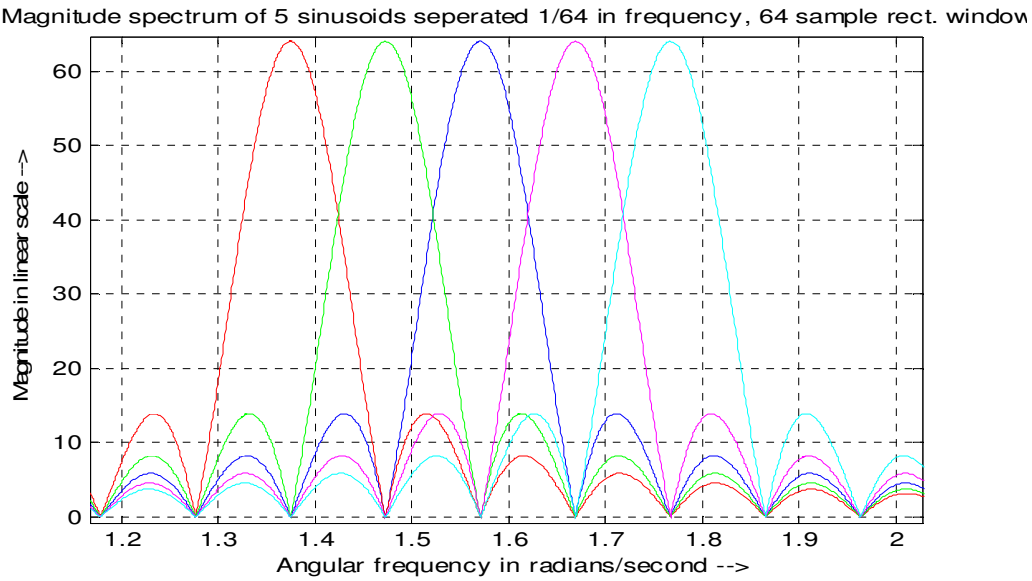

Figure 3: Magnitude spectrum of 5 sinusoids separated by $1/T$ frequency, sampled using length 64 rectangular window

In Figure 3, 5 fractional frequencies corresponding fractional frequency 14 to 18 times 1/64 are shown. It is seen that at the main peak of each of the signals component, all the other signal components are zero. In other words, the signals are orthogonal and do not interfere with each other.

Thus, using this technique, in a sampling window of period *T*, with N samples, N frequency components from –N/2 to N/2-1 can be multiplexed. The bandwidth used would be N/*T* Hz.

2.2 Generation of OFDM signals

Let $\mathbf{x}_f = \left[x_f(0) \quad x_f(1) \quad x_f(2) \ldots \quad x_f(N-1) \right]^+$ be the frequency domain signal to be transmitted, where '+' corresponds to transpose operation. The time domain signal is obtained by multiplying the signal vector with the following matrix

$$\mathbf{x} = \frac{1}{\sqrt{N}} \begin{bmatrix} 1 & 1 & 1 & \cdots & \cdots & 1 \\ 1 & e^{\frac{j\pi}{N}} & e^{\frac{j2\pi}{N}} & e^{\frac{j3\pi}{N}} & \cdots & e^{\frac{j(N-1)\pi}{N}} \\ 1 & e^{\frac{j2\pi}{N}} & e^{\frac{j4\pi}{N}} & e^{\frac{j6\pi}{N}} & \cdots & e^{\frac{j2(N-1)\pi}{N}} \\ \vdots & \vdots & \vdots & \vdots & \ddots & \vdots \\ \vdots & \vdots & \vdots & \vdots & \ddots & \vdots \\ 1 & e^{\frac{j(N-1)\pi}{N}} & e^{\frac{j2(N-1)\pi}{N}} & e^{\frac{j3(N-1)\pi}{N}} & \cdots & e^{\frac{j(N-1)(N-1)\pi}{N}} \end{bmatrix} \mathbf{x}_f$$

It is seen that the above matrix is the Inverse Discrete Fourier Transform (IDFT). If N is made a power of 2, the above operation can be efficiently implemented as an Inverse Fast Fourier Transform (IFFT) operation. The receiver, in order to obtains the signal back in the frequency domain using Fast Fourier transform (FFT).

2.3 OFDM Block Diagram

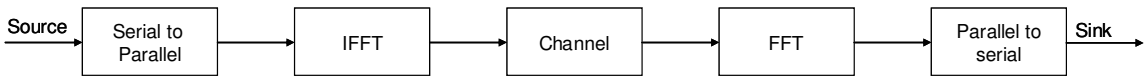

Figure 4: Block diagram for OFDM based communication system

An OFDM based communication system is shown in Figure 4. The incoming data symbols are converted into M ≤ N parallel sub-streams and each of these sub-streams is taken to be signal component in frequency domain. The IFFT operation renders the signal in time domain. The time domain signal is transmitted through the channel. The receiver receives the time domain signal and performs FFT operation to obtain the corresponding frequency domain components. The data is then converted into a serial stream and handed over for further processing.

2.4 IEEE 802.11a/g Physical layer description

IEEE 802.11b has a nominal bandwidth of 20 MHz and operates in the 2.4GHz band and gives a maximum data rate of 11Mbps and uses Direct Sequence Spread Spectrum (DSSS) at the physical layer. IEEE 802.11a was designed to operate in the 5 GHz band with 20

MHz bandwidth. It uses OFDM and provides a maximum rate of 54 MHz. The 802.11g has the similar physical layer as 802.11a at higher data rate but operates in the 2.4 GHz band. It was proposed in order to use the same band as the slower 802.11b standard but give 802.11a like data rates.

802.11a uses 64 point IFFT and FFT operations. However, in order to minimize the window shaping needed to avoid inter channel interference, the first six and the last 5 frequency indices are not used and set to zero during the IFFT operation. Also, to eliminate DC component during sampling operations, the frequency index zero is also not used. A total of 52 frequencies (-26 to -1 and 1 to 26) are available to be used for modulation. Of this, frequency indices -21, -7, 7 and 21 are used as pilot symbols for channel estimation. The remaining 48 symbols can be used for data transmission.

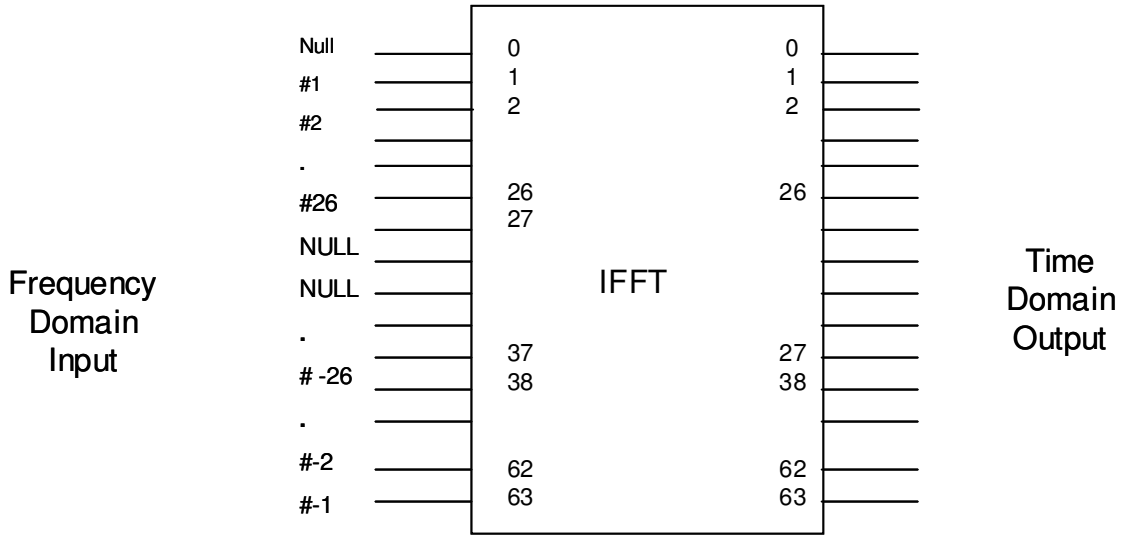

Figure 5: Transmit side frequency domain mapping of symbols

2.5 Terms used in context of 802.11a/g

Symbol: Symbol stands for one full block of time domain data that is obtained after an IFFT operation and addition of cyclic prefix. The FFT is performed on a full received symbol. The 802.11a symbol is shown in Figure 6.

Sub symbol: It is the output obtained in each step of the IFFT operation in the time domain.

Channel: The physical bandwidth occupied by the symbol.

Sub channel: The bandwidth occupied by each frequency component.

Cyclic prefix (CP): In order to maintain the orthogonality of the frequency components in presence of inter symbol interference, a redundant prefix is added to the output of each IFFT operation at the transmitter. This consists of the last 16 sub symbols of a symbol. At the receiver, the first 16 sub symbols corresponding to the cyclic prefix are discarded after timing estimation.

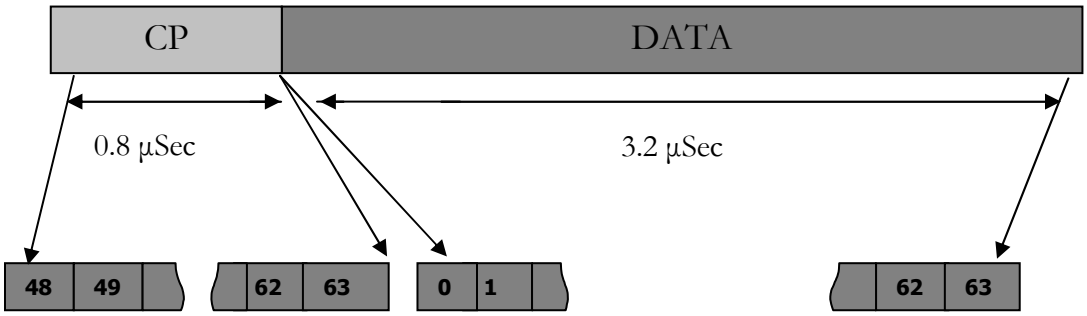

Figure 6: 802.11a/g OFDM Symbol

802.11a/g Frame: An 802.11a/g frame (Figure 7) consists of multiple 802.11a symbols. The first symbol is the short training sequence that is used in timing and frequency synchronization. The second symbol is also a training sequence and is called the long training sequence and can be used to do fine frequency offset estimation and channel estimation. The third symbol is a data symbol that has information such as the number of bits of data, the coding rate, the modulation type and other signaling information. The remaining symbols are data.

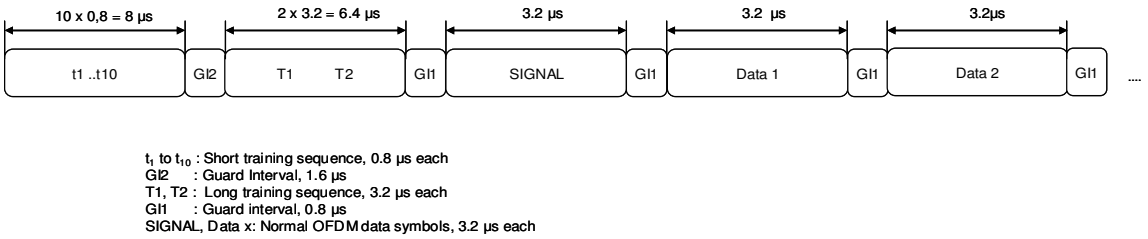

Figure 7: 802.11 a/g OFDM frame structure and timing

Each OFDM symbol has 80 sub symbols and has duration of 4 µsec. Thus, the sub symbol rate is 4/80 = 50 nsec and the bandwidth required is 1/50 nsec = 20 MHz.

802.11a/g support BPSK, QPSK, 16QAM and 64QAM and code rates of 1/2, 2/3 and 3/4. The possible data rate, modulation and coding rate combination are given in Table 1.

Table 1: IEEE 802.11 a/g rate, modulation and coding

Data Rate(Mbps)	*Modulation*	*Coding rate*
6	BPSK	1/2
9	BPSK	3/4
12	QPSK	1/2
18	QPSK	3/4
24	16QAM	1/2
36	16QAM	3/4
48	64QAM	2/3
54	64QAM	3/4

Figure 8 shows a typical transmitter/receiver architecture for a IEEE 802.11a/g system.

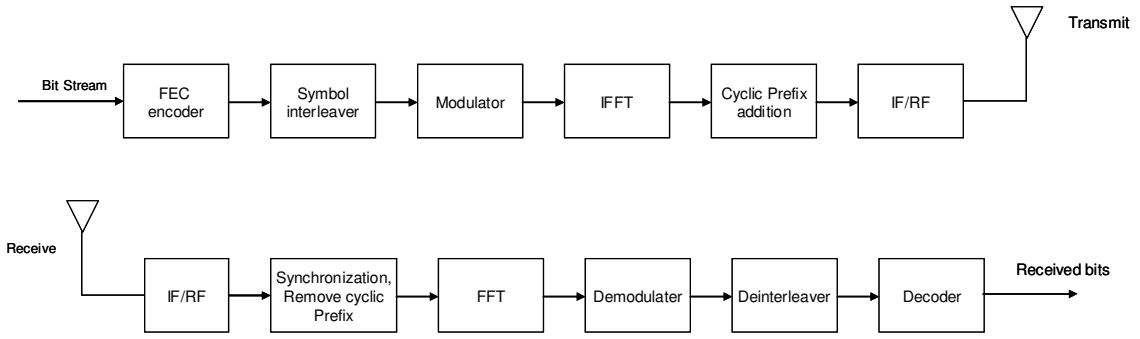

Figure 8: Typical transmitter/receiver architecture for 802.11a/g OFDM system

802.11a/g uses constraint length 7, rate 1/2 convolution encoder. Puncturing is used to obtain the code rates of 2/3 and 3/4.

2.6 Modification proposed by the 802.11 Task group n (TGn):

802.11n promises data rates of 600 MBPS and above exploiting the gains using MIMO algorithms. Some of the other enhancements proposed are use of LDPC codes of rates upto 7/8, use of 400 nano seconds guard intervals instead of 800 nano seconds as in 802.11a/g, use of double the bandwidth (40MHz instead of 20MHz) etc. The proposals are still in the preliminary stage and should be finalized by end 2005.

The main feature in the physical layer in common in the proposals is the use of some sort of per antenna channel sounding. Most proposals also talk about feedback mechanisms to better tailor the modulation type and use of channel sounding. The 802.11n is designed to be backward compatible at both the access point and the user end to 802.11g. So, the number of antennas to be used varies from one to four. Most of the proposals deal with some form of SVD based transmission schemes where the transmitter as well as the receiver has channel information.

The proposal used in this thesis is based on TGn Sync [8], proposed by Agree systems. A typical frame format for the new proposal is shown in Figure 9.

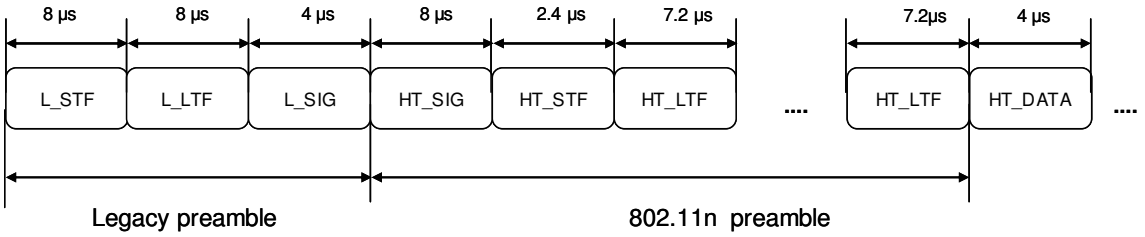

Figure 9: Proposed frame format for 802.11n TGn Sync

Figure 9 shows the basic frame format for the 802.11n. The L stands for the Legacy, which is used to make it backward compatible with 802.11a/g systems. The frame symbol names are explained in Table 2.

Table 2: Symbol names in proposed 802.11n TGn Sync frame

Symbol name	*Symbol function*
L_STF	Legacy short training sequence
L_LTF	Legacy Long training sequence
L_SIG	Legacy signal
HT_SIG	High Throughput signal
HT_STF	High Throughput short training sequence
HT_LTF	High Throughput long training sequence
HT_DATA	High Throughput data

The Legacy Short Training Frame (L_STF) and Legacy Long Training Frame (L_LTF) are the same ass the 802.11a/g short and long training sequences. The main difference is the High Throughput (HT) segments which are specific to the 802.11n TGn Sync proposal.

The High Throughput Shorting Training Frame (HT-STF) is used for timing estimation and signal strength computation. The Channel information is obtained by using the long training sequence in the High Throughput Long Training Frame (HT-LTF). In case of more then one antennas, the tones are interleaved between the transmit antennas so that each transmit antenna transmits a unique set of tones two times. The receive antennas use this to obtain the frequency response of the channel for a set of tones for a particular transmit antennas.

A setup for the case of two transmit antenna and 20 MHz bandwidth is illustrated as an example. The long training sequence frequency domain symbols transmitted from each antenna in a given symbol are a subset of the following sequence.

$$HTL_{-26,+26} = \{-1, 1, -1, 1, 1, 1, -1, -1, -1, -1, 1, 1, 1, 1, -1, 1, -1, 1, -1, -1, 1, 1, 1, -1, 1, 1,$$
$$0, -1, 1, 1, -1, -1, 1, -1, -1, 1, -1, -1, 1, -1, -1, 1, 1, 1, 1, -1, 1, 1, 1, 1, 1, 1, 1\}$$

The index -26 to 26 indicate the frequency index of the data, with a zero at D.C.

The frequency domain symbols are split into the following two groups, where the indices convention of MATLAB is followed.

set_1 = [-26:2:-2], [+2:2:+26]

set_2 = [-25:2:-2],[+1:2:+25]

HTL(set_1) is transmitted from antenna 1 and set HTL(set_2) is transmitted from antenna 2, two times each. The sets are then changed between the antenna and antenna 1 transmits HTL(set_2) and antenna 2 transmits HTL(set_1). Thus, the receiver can get the full channel information from all the transmit antenna in the frequency domain. Figure 10 shows the symbol sequence for the HT_LTF when two antennas are used. GI stands for Guard Interval.

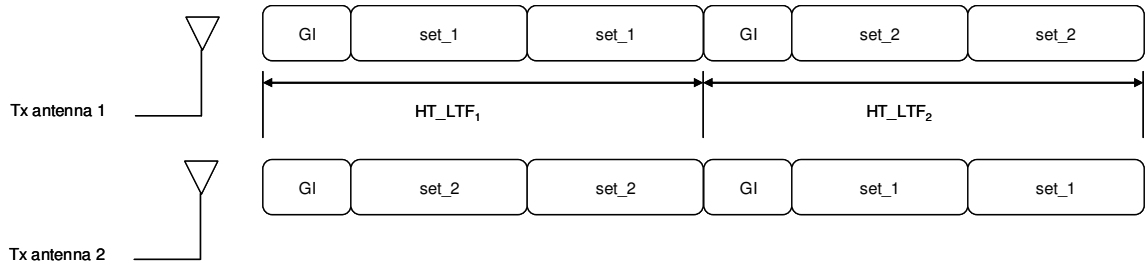

Figure 10: HT-LTF Transmit Scheme for two Transmit Antennas

In cases N transmit antennas, the frequency domain long training sequences are split into indices of N equal groups that is transmitted two time from each antennas.

The typical architecture for a 20MHz channel is similar to a 802.11a/g model shown in Figure 8 but for the fact that there is a spatial multiplexing block at the transmitter and a spatial demultiplexer at the receiver. Figure 11 shows the block diagram for proposed 802.11n TGn Sync two antenna transmit operation.

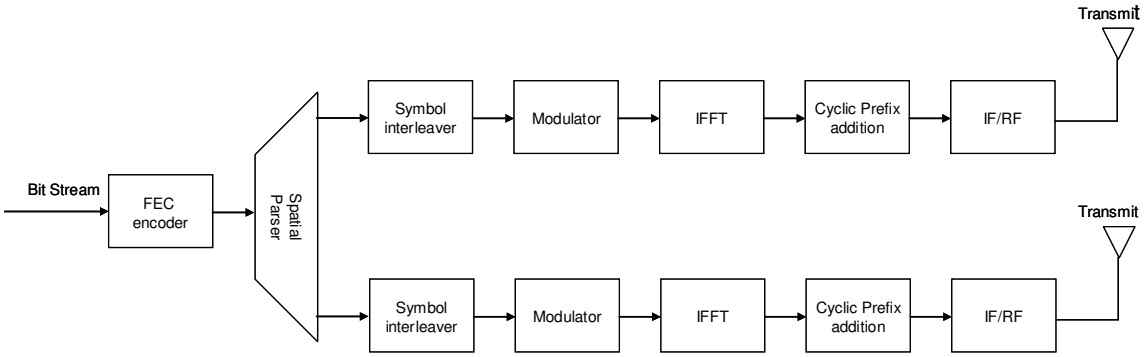

Figure 11: Basic two antenna transmit architecture for 802.11n TGn Sync proposal

The serial data is first split into parallel spatial streams and each spatial stream acts like an independent OFDM transmitter.

The possible modulation, coding rate, bandwidth used and raw decoded data rate for the proposed 802.11n TGn Sync is shown in Table 3.

Table 3: Spatial channels, modulation, code rate and data rate combinations in 802.11n TGn Sync proposal

Number of spatial streams	***Modulation***	***Coding rate***	***GI = 800ns***		***GI = 400ns***	
			Rate in 20MHz	Rate in 40MHz	Rate in 20MHz	Rate in 40MHz
1	BPSK	1/2	6	13.5	6.67	15
1	QPSK	1/2	12	27	13.33	30
1	QPSK	3/4	18	40.5	20	45
1	16QAM	1/2	24	54	26.67	60
1	16QAM	3/4	36	81	40	90
1	64-QAM	2/3	48	108	53.33	120
1	64QAM	3/4	54	121.5	60	135
1	64QAM	7/8	63	141.75	70	157.5
2	BPSK	1/2	12	27	13.33	30
2	QPSK	1/2	24	54	26.67	60
2	QPSK	3/4	36	81	40	90
2	16QAM	1/2	48	108	53.33	120
2	16QAM	3/4	72	162	80	180
2	64QAM	2/3	96	216	106.67	240
2	64QAM	3/4	108	243	120	270
2	64QAM	7/8	126	283.5	140	315
3	BPSK	1/2	18	40.5	20	45
3	QPSK	1/2	36	81	40	90
3	QPSK	3/4	54	121.5	60	135
3	16QAM	1/2	72	162	80	180
3	16QAM	3/4	108	243	120	270
3	64QAM	2/3	144	324	160	360
3	64QAM	3/4	162	364.5	180	405
3	64QAM	7/8	189	425.25	210	472.5
4	BPSK	1/2	24	54	26.67	60
4	QPSK	1/2	48	108	53.33	120
4	QPSK	3/4	72	162	80	180
4	16QAM	1/2	96	216	106.67	240
4	16QAM	3/4	144	324	160	360
4	64QAM	2/3	192	432	213.33	480
4	64QAM	3/4	216	486	240	540
4	64QAM	7/8	252	567	280	630

2.7 Interleaving in 802.11a/g/n

Interleaving is carried out in two stages. The first stage sees to it that the adjacent coded bits are separated by 2 sub channels. This is done so that in case of deep fades in some channels, there is better chance of recovery from bits falling in sub channels that are not affected by the deep fade.

The second stage interleaver sees to it that adjacent bits falls alternately in the most significant portion and least significant portion of the modulate symbol. This is useful in case of 16QAM and 64QAM modulation where the bit errors are more likely to occurs in the bits corresponding to the least significant portion of the symbol and less likely in the most significant portion of the symbol. The second interleaver randomizes the errors in the coded bit stream due to the relative placement of bits in the symbol constellation.

3 Frequency Domain Models of 802.11 based OFDM Systems

In this chapter, a frequency domain based model of 802.11 OFDM is developed. The model is for a Single Input/Single Output (SISO) channel. This model can be used to evaluate and predict the performance of the SISO system in terms of capacity and BER . Also, it forms the groundwork for analyzing the Multi Input/Multi Output (MIMO) systems in the next chapter.

3.1 Equivalent Frequency Domain SISO Channel model

Consider a SISO channel with K resolvable multipath. A single baseband output y_n can be represented as

$$y_n = \sum_{k=0}^{K-1} x_{n-k} h_k + \eta_n$$

where

x_n is the n^{th} input

h_k is the k^{th} channel tap

η_n is the complex AWGN with distribution $N(0, \sigma^2)$

The channel taps are modeled as complex Rayleigh. Measurement campaigns for indoor channels that are summarized in [6] have lead to development of models with clustered reflectors with an exponential decay profile for the taps. An example of a multipath channel with exponential tap decay profile is shown in Figure 12

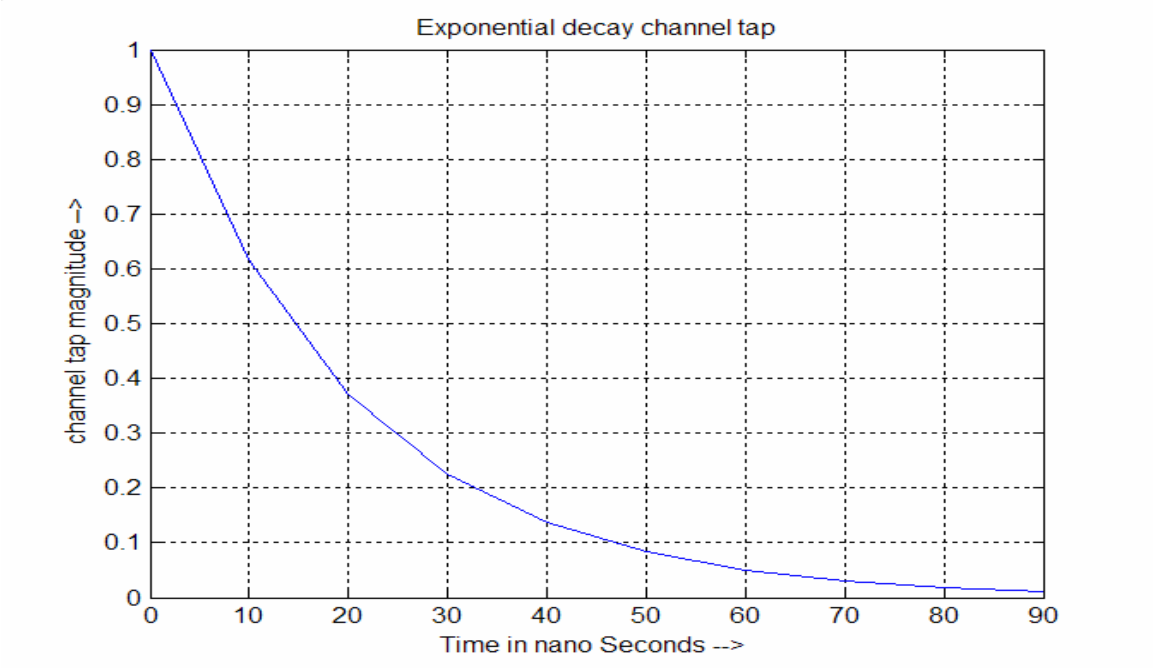

Figure 12: Exponential delay profile channel tap

The sub symbol duration for OFDM is 50 nano seconds and the symbol duration is 4 μ second. A frame may have up to 10 symbols of data and 5 symbol duration for training sequence and header, giving a total time of around 60 μ second. Since the RF environment does not change rapidly in an indoor setting, the channel can be considered quasi static for the period of the frame.

Consider an OFDM symbol of N sub symbols and cyclic prefix P of length less then the last significant tap delay. The output y_n can be expressed in a matrix format as follows:

$$\mathbf{y} = \mathbf{H}\mathbf{x} + \boldsymbol{\eta} \quad \ldots. (1)$$

Where **y** is the received vector, **x** is the transmitted vector and $\boldsymbol{\eta}$ is complex AWGN vector with $N(0,\sigma^2)$ pdf.

$$\mathbf{y} = \begin{bmatrix} y_0 \\ y_1 \\ \vdots \\ y_{N-1} \\ y_N \\ \vdots \\ y_{N+P-1} \end{bmatrix} \qquad \mathbf{x} = \begin{bmatrix} x_0 \\ x_1 \\ \vdots \\ x_{N-1} \end{bmatrix} \qquad \boldsymbol{\eta} = \begin{bmatrix} \eta_0 \\ \eta_1 \\ \vdots \\ \eta_{N-1} \\ \eta_N \\ \vdots \\ \eta_{N+P-1} \end{bmatrix}$$

y and $\boldsymbol{\eta}$ are vectors of N+P length and **x** is of length N.

$$\mathbf{H} = \begin{bmatrix} 0 & 0 & . & . & . & h_0 & 0 & . & . & 0 \\ 0 & 0 & . & . & . & h_1 & h_0 & 0 & . & 0 \\ . & . & . & . & . & . & . & . & . & . \\ 0 & . & . & . & . & h_{K-1} & . & h_0 & 0 & 0 \\ . & . & . & . & . & . & . & . & . & . \\ . & . & . & . & . & . & h_{K-1} & . & h_1 & h_0 \\ h_0 & 0 & . & . & . & . & 0 & h_{K-1} & . & h_1 \\ h_1 & h_0 & . & . & . & . & . & h_{K-1} & . & h_2 \\ . & . & . & . & . & . & . & . & . & . \\ 0 & . & . & . & 0 & 0 & h_{K-1} & . & h_1 & h_0 \end{bmatrix}$$

H the channel matrix with N+P rows and N columns.

Assuming that the last resolvable multipath component h_{K-1} has a delay less then or equal to the period of the cyclic prefix ($K \leq P$), a square matrix **H'** of order N made out of all columns of **H** and rows greater then K is circulant in the taps of h. A circulant matrix has the property that it is diagonalized by an N point Fourier matrix. The columns of the Fourier matrix are eigen vectors for the circulant matrix. H can now be rewritten as

$$\mathbf{H}' = \mathbf{F}^h \mathbf{H}_f \mathbf{F} \qquad \text{….. (2)}$$

F is a FFT matrix of dimension N.

$\mathbf{F}^h$ is the hermetian of **F.**

$\mathbf{H}_f$ is a diagonal matrix of eigen values of **H** with eigenvectors from **F**. The transmitted vector and the received vector is pre-multiplied by FFT matrix and the hermatian of the FFT matrix respectively so that

$$\mathbf{y}_f = \mathbf{F}\mathbf{y} \qquad \text{…. (3)}$$

$$\mathbf{x}_f = \mathbf{F}^h\mathbf{x} \qquad \text{…. (4)}$$

Substituting (2), (3) and (4) in (1)

$$\mathbf{y}_f = \mathbf{F}(\mathbf{F}^h\mathbf{H}_f\mathbf{F})\mathbf{F}^h\mathbf{x}_f + \mathbf{F}\boldsymbol{\eta}'$$
$$= \mathbf{H}_f\mathbf{x}_f + \mathbf{F}\boldsymbol{\eta}'$$

Where $\boldsymbol{\eta}'$ is the part of the noise vector corresponding to rows of $\mathbf{H}'$

Since $\mathbf{H}_f$ is a diagonal matrix, there is now a decoupled relation between $\mathbf{y}_f$ and $\mathbf{x}_f$.

In case of 802.11 based OFDM system, the length of the cyclic prefix is 0.8 μ second and it consists of 16 symbols. Thus, the maximum delay of the multipath component for which the matrix can be made circulant is 0.8 μ second, assuming perfect timing estimation. The value of N is 64 and the value of P is 16.

3.2 Effect of time domain noise in frequency domain

The noise vector $\boldsymbol{\eta}'$ is assumed white in the frequency domain and has a power spectral density of $\sigma^2 = N_0/2$ in case of band pass sampling of the signal.

Since each output of the product $\mathbf{F}\boldsymbol{\eta}'$ is a sum of N complex Gaussian random variable with $N(0, \sigma^2)$, and **F** comes with a scaling factor $1/\sqrt{N}$, using the central limit theorem, the resulting distribution of $\mathbf{F}\boldsymbol{\eta}'$ is also Gaussian $N(0, \sigma^2)$. Thus, we now have an equivalent frequency domain model of the system shown in Figure 13.

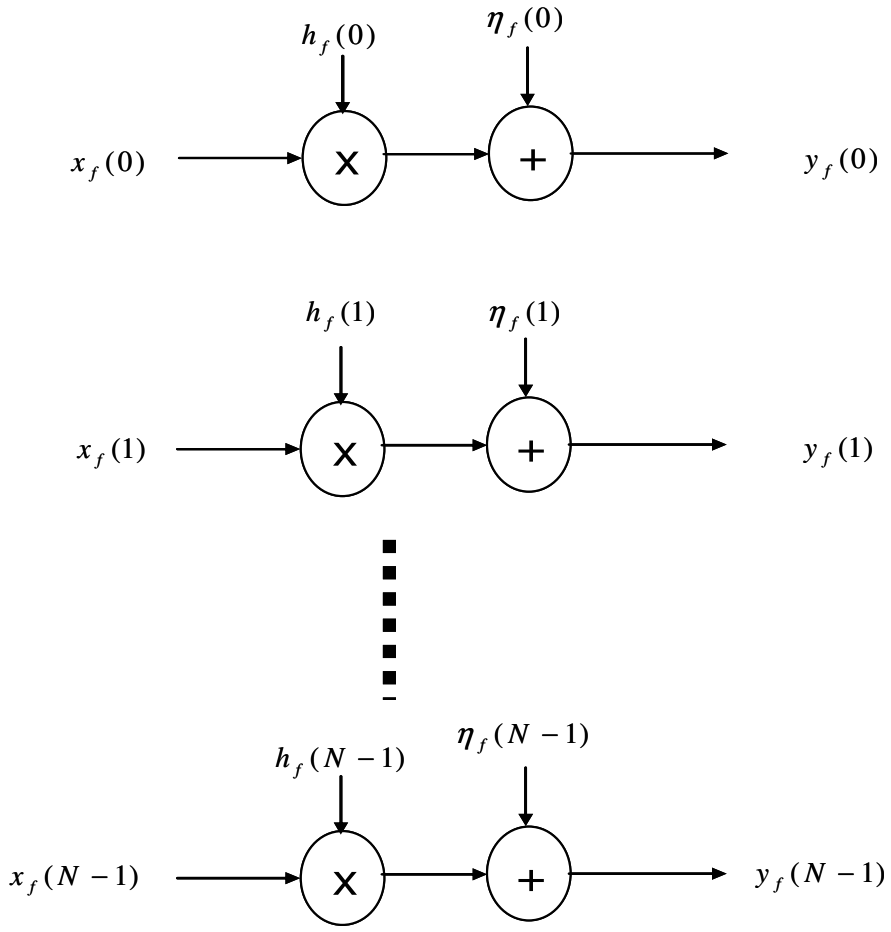

Figure 13: Equivalent flat fading Frequency Domain Channels

$h_f(k)$ are diagonal elements of the N by N matrix H_f and $\boldsymbol{\eta}_\mathbf{f}$ is the equivalent AWGN which has the same $N(0,\sigma^2)$ pdf as the AWGN in the time domain.

The frequency domain model consists of N parallel data symbols that go through N parallel channels with independent flat fading. AWGN is added at the receiver and the symbols are serialized to present the output vector $\mathbf{y}_f$.

This is the frequency domain OFDM SISO model that will be used for simulation purpose in this thesis. In the simulations, an FFT operation is first performed on time domain channel taps assuming perfect timing estimation and no frequency error. The modulated data $\mathbf{x}_\mathrm{f}$ in frequency domain symbols are then multiplied by frequency domain channel

gains obtained from FFT of the channel taps and the noise added to obtain the received frequency domain symbols.

3.3 Computation of Signal to Noise Ratio per Sub Channel:

Consider a single sub channel in the frequency domain model:

$$y_f(k) = x_f(k)h_f(k) + \eta_f(k)$$

Signal to noise ration per sub channel= $\frac{(x_f(k)h_f(k))(x_f(k)h_f(k))^*}{\eta_f(k)\eta_f(k)^*}$

Where the '*' operation denotes the complex conjugate operation

Rearranging the terms

Per channel SNR = $\left|x_f(k)\right|^2 \left|h_f(k)\right|^2 \Big/ \left|\eta_f(k)\right|^2$

The first term on the numerator is the signal power. The second term is the channel gain. The value of channel gain can be greater or less then unity, leading to attenuation or amplification of the signal by the channel.

As mentioned before, it is expected that the channel is static for the duration of the frame and the channel estimation is perfect. Issues like frequency drift and timing jitter are ignored.

From the channel gain and the noise estimate, the expected uncoded Bit Error Rate (BER) for a given modulation type can be analytically computed for a given modulation.

Taking a case of BPSK without coding, the BER probability is given by the expression

$$P_e = Q\left(\sqrt{2E_b^2 / N_0}\right)$$

E_b is the effective energy per bit of at the receiver and $N_0/2 = \sigma^2$ is the power spectral density of the AWGN. In case of 802.11 OFDM, there are 48 data sub channels and average BER would be

$$P_t = \frac{1}{48}\sum_{k=1}^{48} Q\left(\sqrt{2E_b(k)^2/N_0}\right)$$

Assuming the BPSK constellation has unity power, the received power per bit is given by $\left[\left|h_f(k)\right|^2\right]$. Under static channel assumptions and band pass sampling, BER for the frame is

$$P_t = \frac{1}{48}\sum_{k=1}^{48} Q\left(\left|h_f(k)\right|/\sigma\right) \quad \text{..... (5)}$$

Similar expressions for error probability for a given channel can be obtained for other modulation type.

The Q function is not easy to evaluate under real time cycle constraints, more so in 802.11 OFDM systems where the symbol duration is in micro seconds. A look up table giving the BER values for a given SNR can be used instead. A simple linear interpolation can be used to obtain the BER value for a given SNR.

The idea is illustrated using a SISO channel with taps as shown in Figure 14. A table was generated for BER in case of BPSK in AWGN channel for linear SNR values ranging from 0.25 to 10. The channel has frequency domain channel gains shown in Figure 15. Computed values of BER using equation (5), simulated values using a million bits and the BER values obtained by using the table are shown in Figure 16. It seen from Figure 16 that all three BER plots are similar and hence, the lookup table based BER computation is feasible.

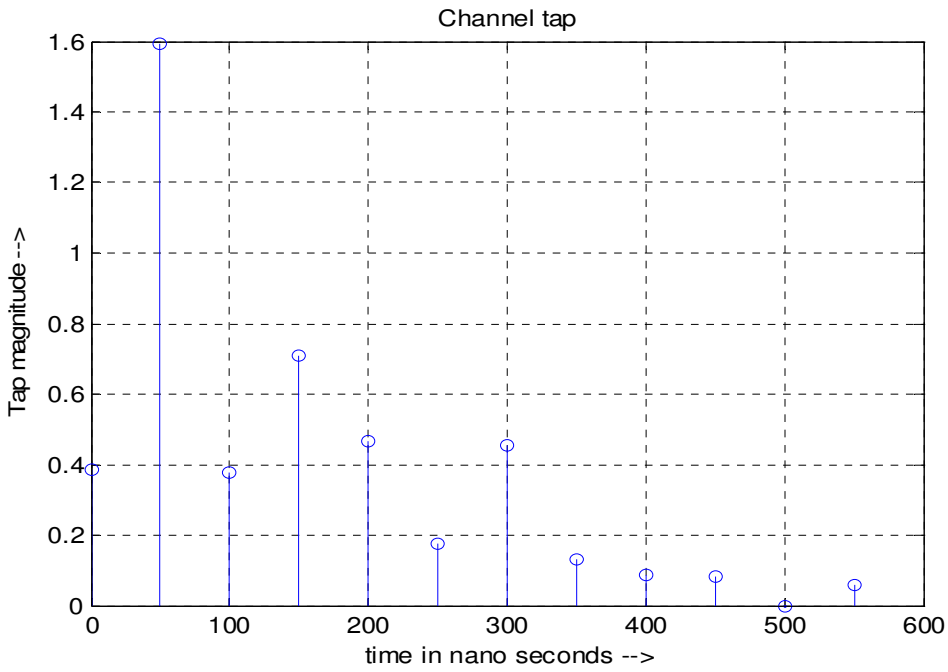

Figure 14: Time domain channel taps used in the example

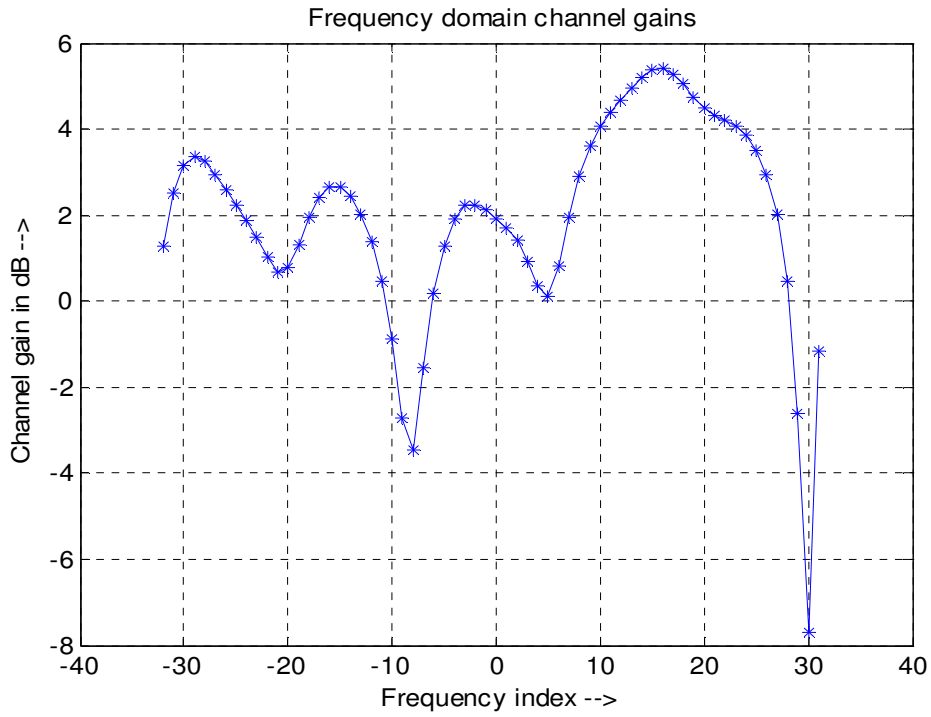

Figure 15: Frequency domain response of the given channel

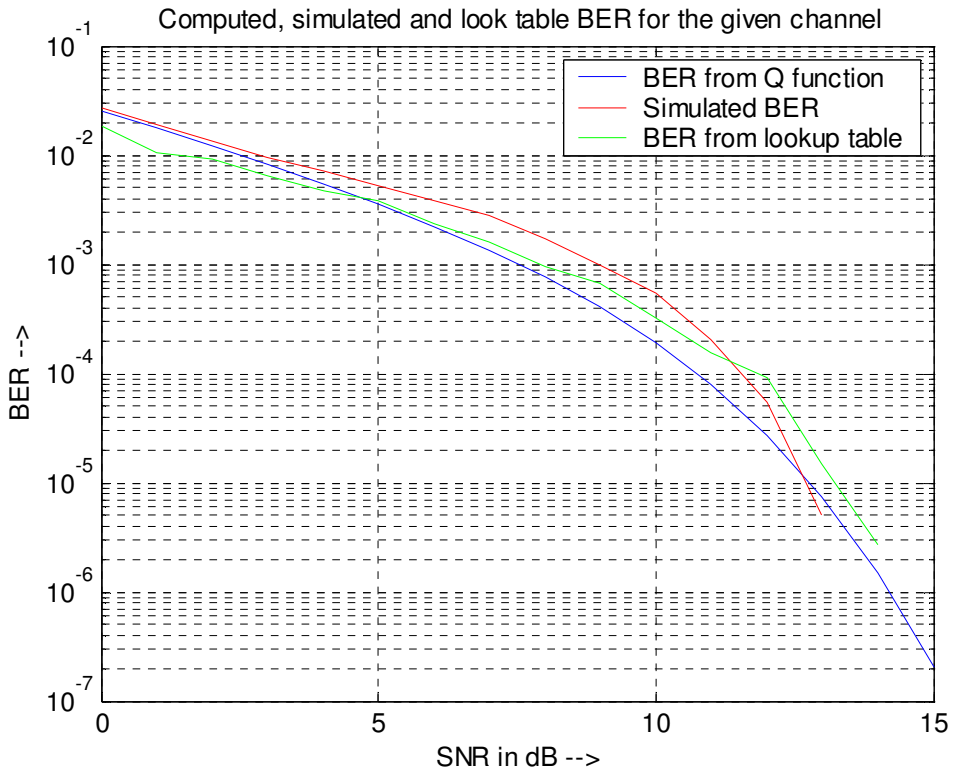

Figure 16: BER performance of 802.11 OFDM BPSK from simulation, Q function and lookup table

3.4 Performance considering channel coding and interleaving:

802.11 OFDM uses a constraint length K = 7, rate ½ convolution encoder with optional puncturing for rates 2/3 and ¾ . The code used is the industry standard $(171)_8$ and $(133)_8$. This code has a free distance (d_{free}) of 10.

The interleaver randomizes the error due to frequency selective fading as well as the relative position of the bits in the symbol constellation. The coded bits received are deinterleaved before decoding.

The most common forms of decoding convolution encoded data is the Viterbi decoder. The decoder is classified into the hard decision decoder or soft decision decoder and is based on the distance metrics used to determine the most likely path. The hard decision decoder uses Hamming distance and is easy to implement in a processor because it involves logical operations. The soft decision decoder uses the Euclidian distance and gives better coding

gain than the soft decision, but is more computation intensive because of the use of arithmetic operations. Hard decision decoding is used in all the simulations.

In case of simple BPSK and AWGN, the performance of bits with the above coding is well known. Coding theory text books [3] give good upper bounds for error probability given the probability of error of the received bits. In case of hard coding and the code considered above, a close bound for error probability is given by

$$P_b = \left(4p(1-p)\right)^{d_{free}/2} \quad \ldots(6)$$

where

P_b is the probability of error for the decoded bit

p is the probability of error for the received coded bit

d_{free} is the free distance for the given code.

But the above formula does not take into consideration the effects of interleaving and sub channels with different channel gains. Thus, it is not possible to compute the expected bit error rate using the above expression directly.

But in a WLAN application, it is sufficient to know if for a given modulation and coding, the bit error rate is below a threshold value. It could be done if an effective SNR that gives the same BER as the BER of the overall channel can be found. A possible way of doing this is the lookup table discussed before, but in the reverse direction. Since the average BER is known, it is possible to find an effective SNR value from the table which would give the same BER as the average BER of the whole system.

In Figure 17, simulation was carried out using the SISO channel in Figure 14 using uncoded BPSK. The equivalent SNR was computed from the table for each average BER values from simulations in different SNR and the BER computed from this using the Q function. It was found to match closely with the simulated BER and BER computed from (5).

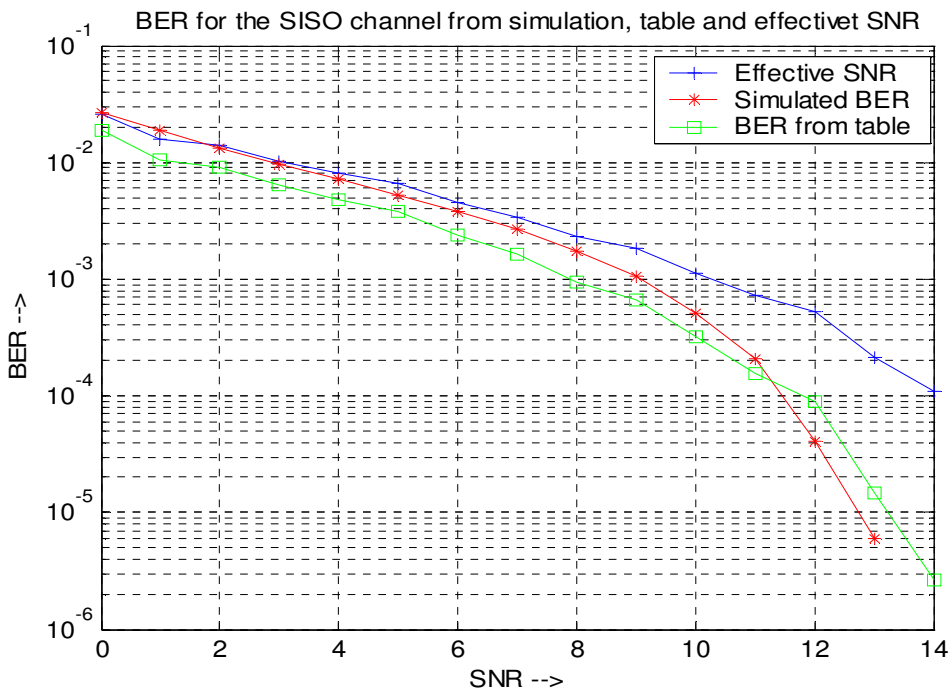

Figure 17: BER for given channel computed from different method

The uncoded bit error rate from effective SNR can be used to compute the coded error rate using the equation (6). Figure 18 shows the BER performance for the SISO channel in Figure 14 when rate ½ code with BPSK is used. It is seen that the BER from the simulation matches the computed BER performance.

The effective SNR can be considered a good parameter to gauge the BER performance of the system. Similar results can be obtained for other combinations of modulation and coding.

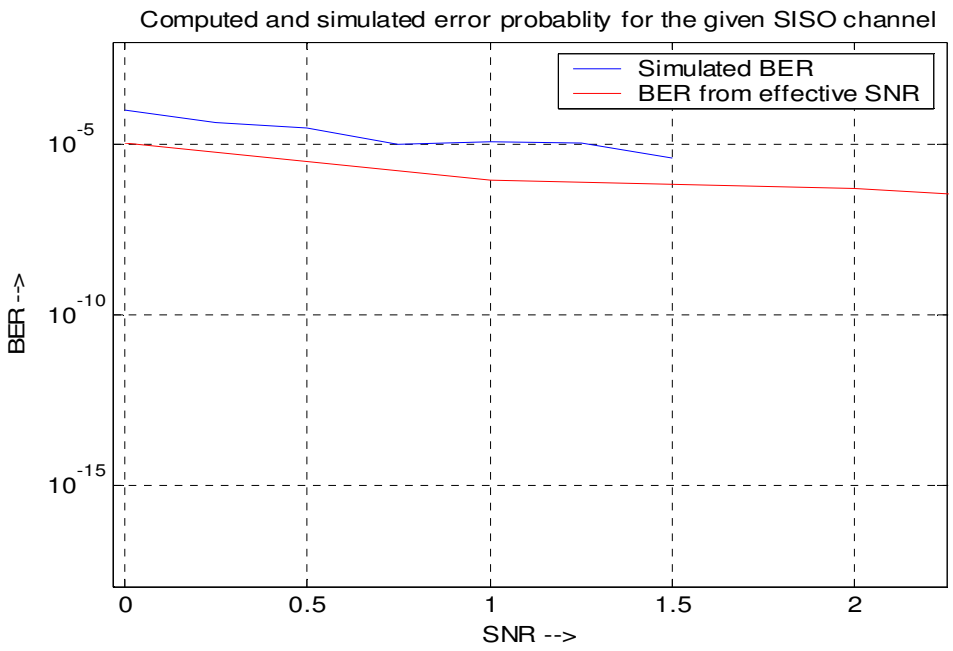

Figure 18: Coded BER for the given SISO channel

Since 802.11a/g uses 4 modulation types, a look up table can be constructed for each of the modulation that gives the BER-SNR combinations. The range and resolution of the table for each modulation type is given in Table 4. The SNR range is in linear scale.

Table 4: SNR-BER table range and resolution

Modulation	*Start SNR (Linear)*	*End SNR (Linear)*	*SNR resolution (Linear)*
BPSK	0.0	10.0	0.25
QPSK	1.0	15.0	0.5
16QAM	1.0	99.5	0.5
64QAM	2.0	318.0	2.0

3.5 BER requirements for the wireless data applications

BER requirements for wireless data is based on the application layer requirements. Streaming applications usually can tolerate bad BER where as applications such as TCP and FTP are far less tolerant because of retransmission of corrupted packets.

A good lower bound for Packet Error Rate (PER) for a low values of BER is given by the expression

$$P_p = 1 - (1 - P_b)^{N_b} \quad \ldots. (7)$$

Where

P_p is the packet error probability.

P_b is the bit error probability

N_b is the number of bits per packet.

For example, for a bit error rate of 10^{-5} and taking a packet of 256 bit length, the packet error rate (PER) from (7) works out to 0.0026, which is 2.6 packets error per thousand packets.

3.6 Modulation and coding selection strategy based on effective SNR

In the previous sections, it was shown that the effective SNR computed from the table gives a good measure of the BER performance of the system in a given channel condition. The assumption here is that a flat fading channel with the effective SNR would give the same BER as given by the frequency selective channel.

With good interleaving, the error probability of the coded bits in a frequency selective fading channel can be assumed to be random. A coded flat fading channel and effective SNR would have the same BER performance as a coded and interleaved system in frequency selective fading. With this assumption, the effective SNR can now be used to predict the BER performance of the coded system. The BER performance of the coded system under AWGN can be pre computed and the required thresholds to achieve a given BER can be found.

In Figure 19, the BER plot for the rates described in Table 1 are plotted. Two sample target BER values of 10^{-5} and 10^{-3} are used to obtain the threshold values shown in Table 5.

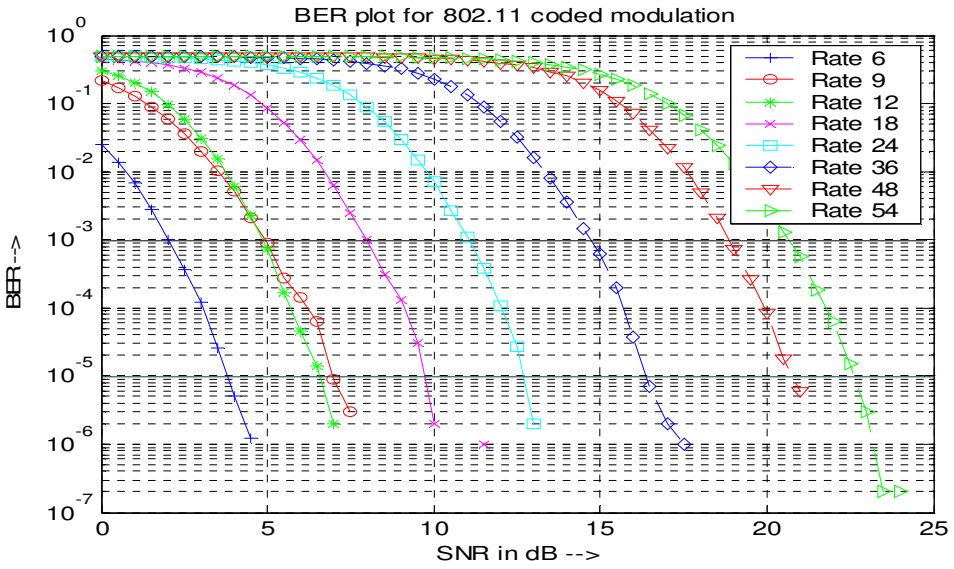

Figure 19: Simulated BER Plot for the 8 rates

Table 5: Threshold effective SNR for rate selection in 802.11a/g

Rate in MBPS	*Threshold of BER 10^{-3}*	*Threshold of BER 10^{-5}*
6	2.0	3.8
9	4.9	7.0
12	5.0	6.6
18	8.0	8.7
24	11.1	12.7
36	14.7	16.4

48	19.8	20.8
54	20.6	27.7

For the SISO channel used in the previous example, the above threshold was used to determine the possible data rates under different SNR with target BER value of $10^{-5.}$ The resultant rate selection is plotted in Figure 20.

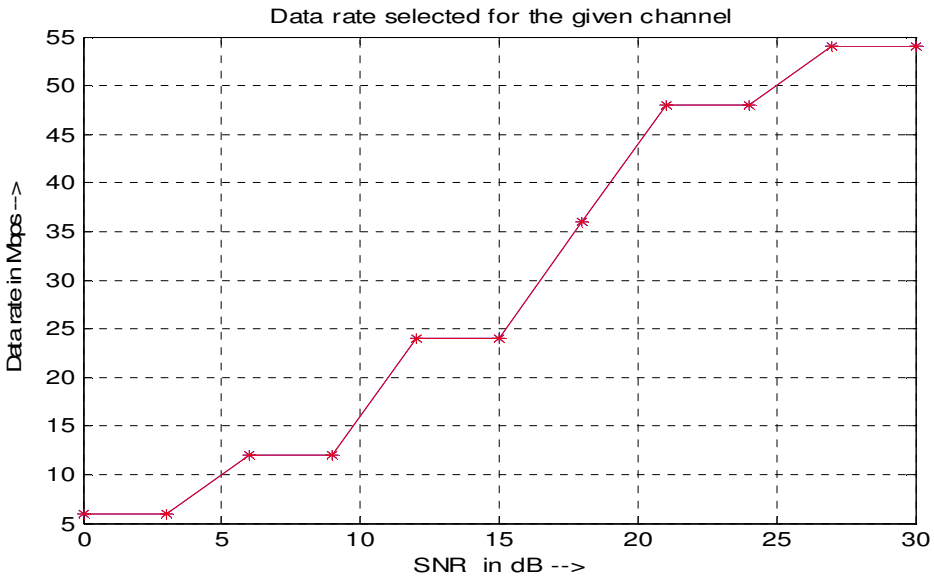

Figure 20: Rate selection for the SISO channel

3.7 Summary of Chapter 3

In this chapter, the parallel, flat fading, frequency channel model for a frequency selective OFDM SISO channel was developed. Using this model, it was shown that a SNR-BER table can be used to compute the BER and the effective SNR can be computed from it. The concept of effective SNR was introduced for the purpose of predicting the BER of coded and interleaved data in a frequency selective channel. It was also seen that the effective SNR can be used as a threshold for rate selection. In the next chapter, the SISO parallel channel model and effective SNR concept is applied to MIMO channels.

4 MIMO In OFDM Systems

Multiple Input Multiple Output (MIMO) systems use multiple transmit and receive antennas to improve the capacity of the system. Some of the common techniques used are the BLAST, Space Time Coding, etc. This chapter discusses the Singular Value Decomposition (SVD) technique to decouple the channel matrix in spatial domain in a way similar to the DFT decouples the channel in the frequency domain. This chapter initially deals with flat fading channel without multipath and then applies the technique in a multipath OFDM system.

4.1 Basic MIMO Channel Matrix

Consider a Transmit/Receive system with T transmit antennas and R receive antennas as shown in the Figure 21 below. For the initial discussion, it is assumed that the channel is flat fading and there is no multipath

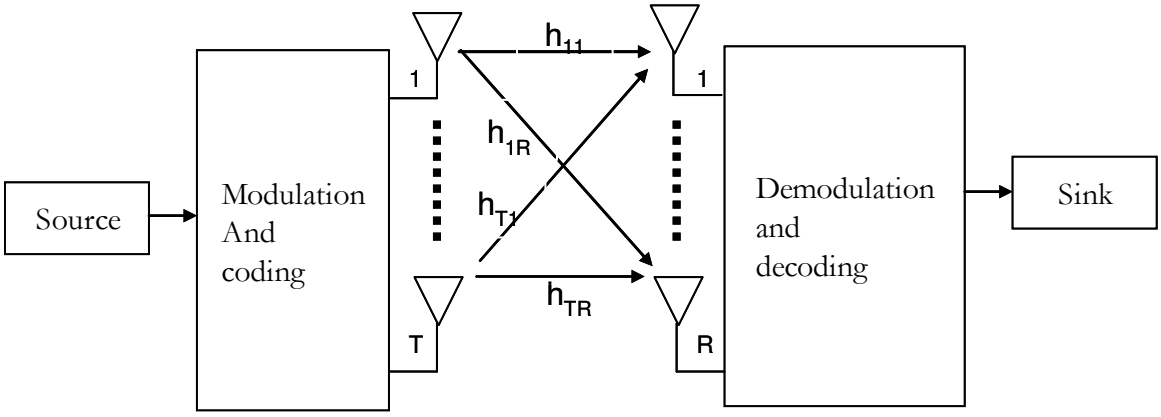

Figure 21: MIMO Channel

Let h_{tr} be the channel coefficient between the t^{th} transmit antenna and r^{th} receive antenna.

Let $\mathbf{x} = [x_1 \quad x_2 \quad \dots \quad x_T]^+$ be the transmitted data and $\mathbf{y} = [y_1 \quad y_2 \quad \dots \quad y_R]^+$ be the received data. '+' stands for transpose operation. In matrix form, the relation between **x** and **y** is given by

$$\begin{bmatrix} y_1 \\ y_2 \\ \vdots \\ y_R \end{bmatrix} = \begin{bmatrix} h_{11} & h_{21} & \cdots & h_{T1} \\ h_{12} & h_{22} & \cdots & h_{T2} \\ \vdots & \vdots & \vdots & \vdots \\ h_{T1} & h_{T2} & \cdots & h_{TR} \end{bmatrix} \begin{bmatrix} x_1 \\ x_1 \\ \vdots \\ x_T \end{bmatrix} + \begin{bmatrix} \eta_1 \\ \eta_2 \\ \vdots \\ \eta_R \end{bmatrix}$$

or

$$\mathbf{y} = \mathbf{Hx} + \boldsymbol{\eta}$$

Where $\boldsymbol{\eta}$ is the complex AWGN vector with pdf $N(0,\sigma^2)$.

H is the T x R channel matrix. If H has independent rows and columns, Singular Value Decomposition (SVD) yields

$$\mathbf{H} = \mathbf{U}\sum\mathbf{V}^h$$

Where $\mathbf{U}$ and $\mathbf{V}$ are unitary matrices and $\mathbf{V}^h$ is the hermitian of $\mathbf{V}$

$\mathbf{U}$ has dimensions of R x R and $\mathbf{V}$ has dimensions of T x T.

$\sum$ is a T x R matrix. If T = R, it is a diagonal matrix. If T > R, it is made of R x R diagonal matrix followed by T – R zero columns. If T < R, it is made of T x T diagonal matrix followed by R – T zero rows.

This operation is called the singular value decomposition of **H**. Any non singular matrix can have singular value decomposition which leads to non zero minimum of (T,R) diagonals.

The case of T = R = T is analyzed first. In this case $\sum$ can written as

$$\sum = \begin{bmatrix} \delta_1 & 0 & \cdots & 0 \\ 0 & \delta_2 & \cdots & 0 \\ \vdots & \vdots & \ddots & \vdots \\ 0 & \cdots & 0 & \delta_T \end{bmatrix}$$

Suppose the **x** is pre multiplied with a matrix **V** and Y is pre multiplied with $\mathbf{U}^h$, the following expression results

$$\mathbf{z} = \mathbf{U}^h \mathbf{y}$$
$$= \mathbf{U}^h (\mathbf{HVx} + \boldsymbol{\eta})$$
$$= \mathbf{U}^h \mathbf{U} \sum \mathbf{V}^h \mathbf{Vx} + \mathbf{U}^h \boldsymbol{\eta}$$
$$= \sum \mathbf{x} + \mathbf{U}^h \boldsymbol{\eta}$$

Since the matrix $\sum$ is a diagnolized matrix, the relationship between **z** and **x** can be decoupled into the form

$$y_t = \delta_t x_t + \eta_t$$

This can be viewed as T parallel flat fading channels. The scheme that uses the above concept is explained below.

The SVD based transmit scheme is shown in Figure 22. The spatial parser splits the symbols into spatial streams. The streams are then multiplied by the columns of **V** to obtain the symbols to be transmitted by each antenna.

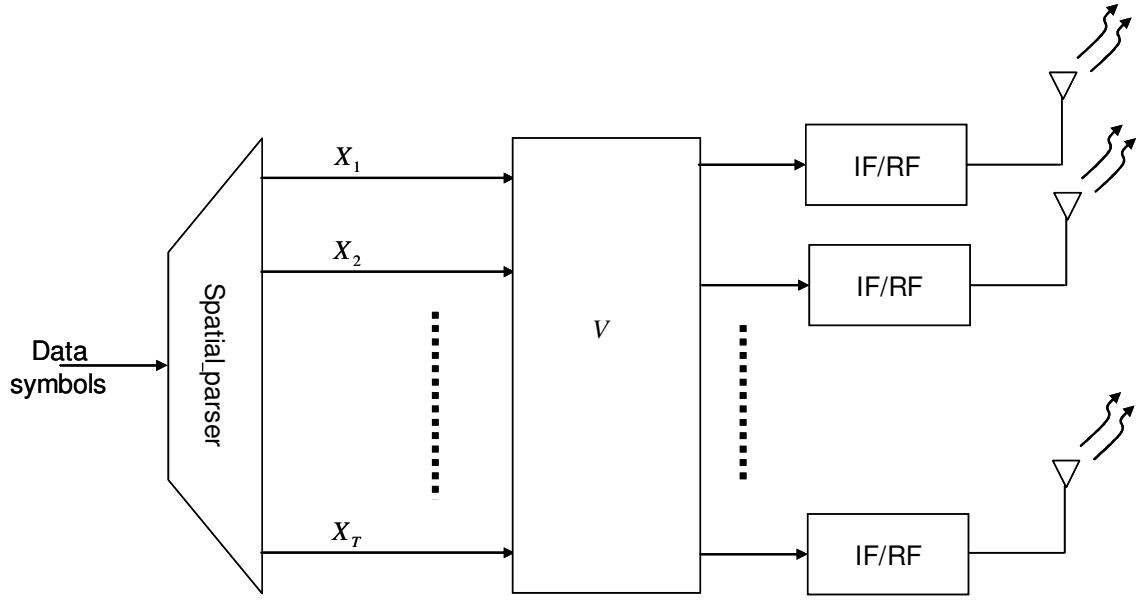

Figure 22: SVD based MIMO transmitter

The receiver for the above transmitter is shown below. In the receiver, the received signals are multiplied by the matrix $\mathbf{U}^h$ to separate out the spatial streams of data and the resultant symbols are combined in the spatial combiner.

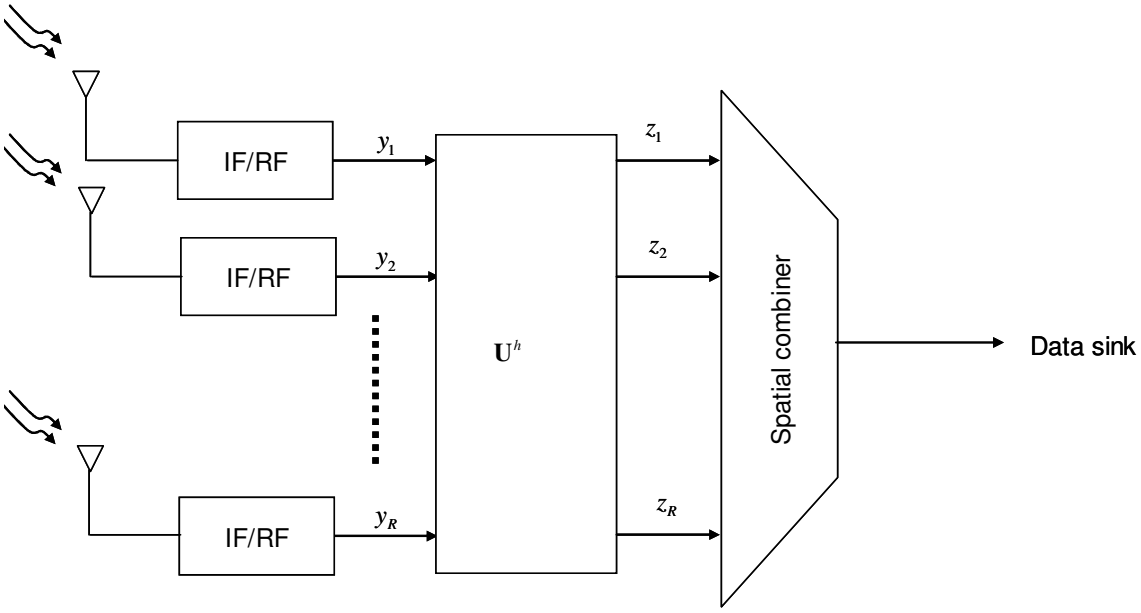

Figure 23: SVD based MIMO receiver

4.2 Developing Equivalent Parallel Flat Fading Model

As done in chapter 3, it is easy for simulation and capacity computation if the system can be reduced to a model with parallel, flat fading paths. Again, the diagonal matrix $\sum$ proves useful.

Since $\sum$ is a diagonal matrix, **z** can now be written as

$$z_t = \delta_t x + \sum_1^R u_{tr}^h \eta_t$$

The columns of the matrix **U** describe a T dimensional space. As in the case of spectral decomposition, the AWGN can be assumed to be spatially white if three is no correlation between the column vectors of **U** and noise vector $\boldsymbol{\eta}$. Applying the central limit theorem,

$$z_t = \delta_t x_t + \eta_t$$

where η_t is AWGN with the same $N(0,\sigma^2)$ distribution in the receiver, but in the spatial domain.

A way of looking at this is that T parallel streams of data are transmitted in orthogonal spatial channels. As in the case of OFDM, an equivalent parallel flat fading model can be used for analysis and simulation.

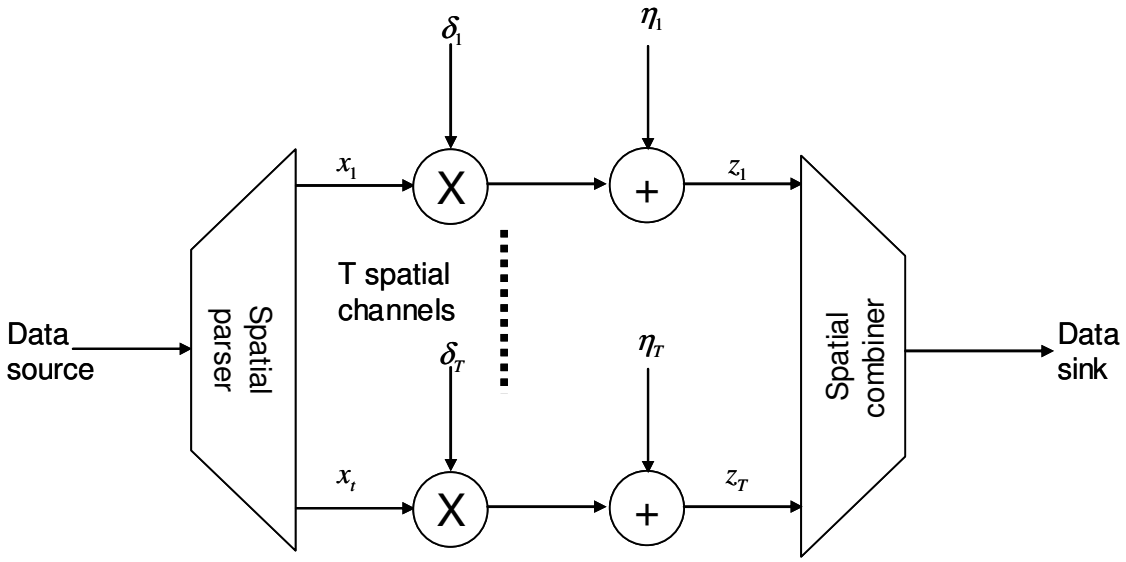

Figure 24: Equivalent Parallel Spatial with flat fading

δ_t is treated as the spatial channel gain and can be used to estimate the BER at the receiver.

As in Chapter 3, assuming coherent detection where the value of δ_t is known, the SNR at the receiver is given by

$$SNR = \frac{|x_t|^2 |\delta_t|^2}{|\eta_t|^2}$$

Assuming a channel that is static and a constant modulo signal as in BPSK, the SNR per spatial channel is

$SNR = \delta_t^2 / \eta_t^2$

The bit error can be computed as

$$P_t = Q\left(\frac{\delta_t}{\sigma}\right)$$

σ comes from the pdf η_t being $N(0, \sigma^2)$

P_t is the bit error probability for a particular spatial channel.

The overall error probability is given by

$$P_{average} = \frac{1}{T}\sum_{1}^{T} P_t$$

δ_t can be seen as the channel gain of the spatial channel t.

A flat fading 4x4 MIMO channel was generated for a Uniform Linear Array (ULA) with correlation properties as described in Appendix 1. δ_t values were obtained using the SVD function in matlab and are as shown below.

$\delta_1 = 1.83514108105847$

$\delta_2 = 0.49193260469410$

$\delta_3 = 0.13044557968295$

$\delta_5 = 0.02833800461830$

The spatial channel gains were used to get the BER curves for uncoded BPSK modulation on per channel basis and over all the channels by BPSK by simulation and computation. The BER plots are shown in Figure 25 and Figure 26

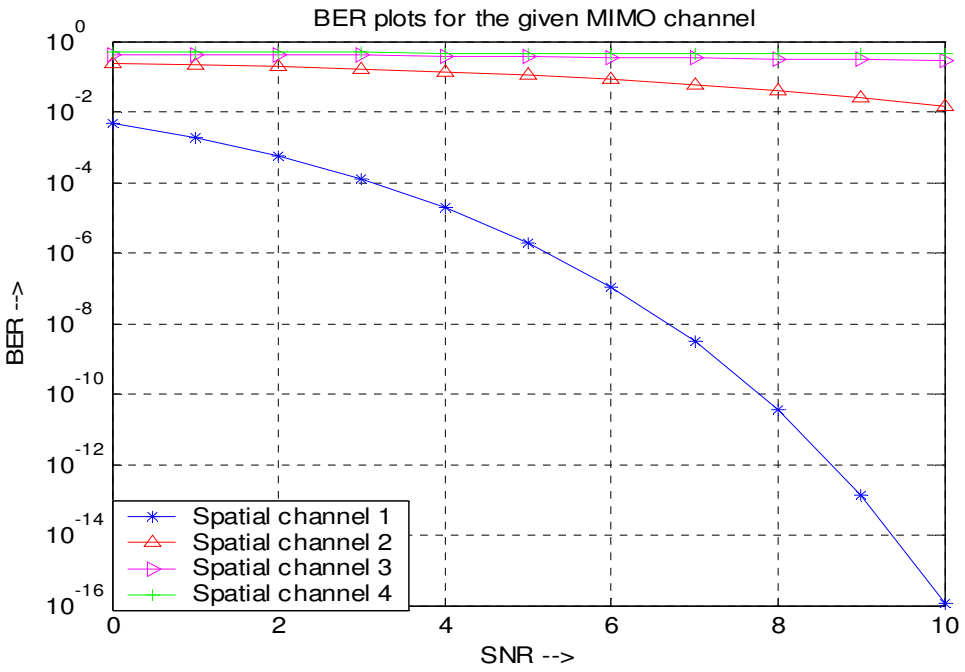

Figure 25: BER Plots for Different Spatial channels for BPSK in AWGN

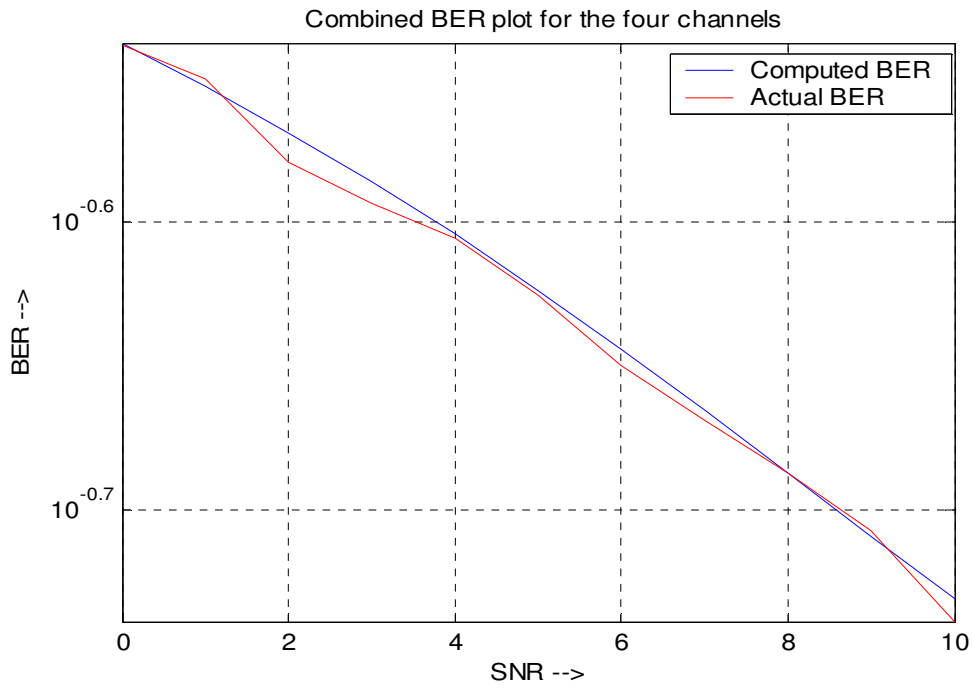

Figure 26: BER plot when all the channels are combined

It is seen that spatial channel 1, which has the highest spatial channel gain ($\delta_1 = 1.8$) , has the best BER performance. Conversely, the worst BER performance is from spatial channel 4, which has the lowest channel gain ($\delta_4 = 0.02$).

As in case of OFDM channels, it is useful to look at what happens when coding and interleaving is included. At low SNR values, spatial channels with weak gains would fail with high probability and can be treated as the code being punctured. In this case, since three of the four channels are weak, the effective puncturing rate would be ¼. Assuming a coding rate of ½, it is seen that the puncturing rate is greater then coding rate and hence there is no redundancy and no coding gain.

Taking the packet rate into picture, using all four spatial channels would result in greater packet error rate and resultant loss of data throughput. In cases where one or more of the spatial channels are bad, it is better not to use the spatial channel.

4.3 Water filling and bit loading

Water filling refers to the technique wherein the powers for the spatial channels are adjusted based on the channel gains. The channel with high gain is given more power. In OFDM systems, this is not generally implemented because it could worsen the inherent OFDM issue of high peak to average power ratio.

Bit loading, on the other hand, increases the number of bits per symbol sent in the spatial channel with high gain. This is could be done by either increasing the coding rate and/or changing the modulation. A table can be generated as in the case of OFDM SISO channel in chapter 3 and a selection can be made based on the channel gain of the spatial channel and the SNR conditions. The disadvantage of this approach is that it increases the complexity in the receiver because the receiver has to do demodulation and decoding in different channels.

4.4 Channel capacity view of SVD MIMO

Limits of channel capacities for MIMO systems was first formulated by Gans and Foschini in the paper [9]. The expression is given by

$$C = \log\left(\det\left(\mathbf{I}_T + \frac{SNR}{T}\mathbf{H}\mathbf{H}^h\right)\right) \text{b/Hz}$$

Where $\mathbf{I}_T$ is an identity matrix of dimension T, T is the number of transmit antennas, SNR is the signal to noise ratio and $\mathbf{H}$ is the channel matrix.

Rewriting $\mathbf{H}\mathbf{H}^h$ using SVD

$$\mathbf{H}\mathbf{H}^h = \mathbf{U}\sum\mathbf{V}^h(\mathbf{U}\sum\mathbf{V}^h)$$
$$= \mathbf{U}\sum\mathbf{V}^h\mathbf{V}\sum^h\mathbf{U}^h$$
$$= \mathbf{U}\left|\sum\right|^2\mathbf{U}^h$$

Substituting in expression for channel capacity,

$$C = \log_2\left(\det\left(\mathbf{I}_T + \frac{SNR}{T}\mathbf{H}\mathbf{H}^h\right)\right)$$
$$= \log_2\left(\det\left(\mathbf{U}\mathbf{I}_N\mathbf{U}^h + \frac{SNR}{T}\mathbf{U}|\Sigma|^2\mathbf{U}^h\right)\right)$$
$$= \log_2\left(\det\left(\mathbf{U}\left(\mathbf{I}_T + \frac{SNR}{T}|\Sigma|^2\right)\mathbf{U}^h\right)\right)$$
$$= \log_2\left(\det(\mathbf{U})\det(\mathbf{U}^h)\det\left(\mathbf{I}_N + \frac{SNR}{N_t}|\Sigma|^2\right)\right)$$

The product $\det(\mathbf{U})\det(\mathbf{U}^h) = 1$

The last determinant is a of a diagonal and it is given by the product of the diagonal

$$\det\left(\mathbf{I}_N + \frac{SNR}{T}|\Sigma|^2\right)$$
$$= \left(1 + \frac{SNR}{T}\delta_1^2\right)\left(1 + \frac{SNR}{T}\delta_2^2\right)\ldots\left(1 + \frac{SNR}{T}\delta_T^2\right)$$

Taking log we get the expression for channel capacity as

$$C = \log_2\left[\left(1 + \frac{SNR}{T}\delta_1^2\right)\left(1 + \frac{SNR}{T}\delta_2^2\right)\ldots\left(1 + \frac{SNR}{T}\delta_T^2\right)\right]$$
$$= \log_2\left(1 + \frac{SNR}{T}\delta_1^2\right) + \log\left(1 + \frac{SNR}{T}\delta_2^2\right) + \ldots + \log\left(1 + \frac{SNR}{T}\delta_T^2\right) bits/Hz$$

In this expression, it is seen that when $\frac{SNR}{T}\delta_t^2 << 1$, the expression $\log_2\left(1 + \frac{SNR}{T}\delta_t\right)$ tends to approach zero, and there is no significant gain in capacity by using that spatial channel. Thus, by not using the channel with low capacity, the capacity of the overall system is not reduced significantly.

The above derivation also suggests a way of evaluating the performance of the channels. If the factor $\frac{SNR}{T}\delta_t$ is below a threshold, it is better to leave out the spatial channel. The

number of spatial streams used is less then the maximum number available, but the effective through put could still be enhanced as we shall demonstrate in the next chapter.

When using only Q < T spatial paths, the columns corresponding to the strongest spatial channel gains in matrices **U** and **V** are used. T – Q spatial channels not in use have the corresponding x_t set to zero.

4.5 Case of T ≠ R

In case where T ≠ R, the number of spatial channels become restricted to the minimum of T, R. In case where the number of transmit antennas is greater then the receive antennas (T > R), **U** will be an R x R matrix, **V** will be a T x T matrix and $\sum$ will be made of a square matrix of order R followed by T-R zero columns as shown below.

$$\sum = \begin{bmatrix} \delta_1 & 0 & \cdots & 0 & 0 \cdots 0 \\ 0 & \delta_2 & \cdots & 0 & 0 \cdots 0 \\ \vdots & \vdots & \ddots & \vdots & \vdots \ddots \vdots \\ \underbrace{0 \quad \cdots \quad 0 \quad \delta_R}_{R} & & & & \underbrace{0 \cdots 0}_{T-R} \end{bmatrix}$$

In this case, the matrix **V** has only T-R usable rows corresponding to the T spatial channels. The first T-R elements of transmit vector **x** are used and the others are zeroed out.

An extreme case of this is when there is only one receiving antenna and there are T transmit antennas. In this case, there is only one spatial channel possible. This would be the case when the receiver is a legacy system (may be running 802.11a/g) and the transmitter is the new 802.11n system. The receiver will in this case have a **U** that is a 1 x 1 matrix and only one column of **V** is used as a sort of beam steering weights.

The second case corresponds to when there are more receive antennas then transmit antennas (R < T). In this case, as before, **V** is a T x T matrix, **U** is an R x R matrix and $\sum$ is a TxR matrix with a diagonal matrix of T followed by R-T zero rows as shown below.

$$\sum = \begin{bmatrix} \delta_1 & 0 & \cdots & 0 \\ 0 & \delta_2 & \cdots & 0 \\ \vdots & \vdots & \ddots & \vdots \\ 0 & \cdots & 0 & \delta_T \\ 0 & 0 & \cdots\cdots & 0 \\ \vdots & \cdots & \ddots & \vdots \\ 0 & 0 & \cdots\cdots & 0 \end{bmatrix}$$

An extreme case is when there is only single transmit antenna and R receive antennas. This case would arise when the transmitter is a legacy system and the receiver is 802.11n.

It will be shown in chapter 5 that the multiple transmit/receive antenna based 802.11n system does show gain in the throughput rate in case of legacy systems that use IEEE 802.11a/g with single antennas.

4.6 OFDM and MIMO

In the previous discussion, it was assumed that there is no resolvable multipath and hence the channel was flat fading. This is a good assumption in case where the symbol rate is slow and all the multipath components arrive within duration of the symbol. The V-BLAST architecture proposed in [11] belongs to this category. But the symbol rate of 802.11 OFDM is of the order of 50 nano seconds. The system operates in indoor environments where the multipath delay times are in the same order or more. These conditions make it necessary to take multipath into consideration. As before, in case of SISO OFDM channels, cyclic prefix in the guard intervals can be used to overcome effects of multipath. This resulting narrow band sub channels with flat fading can then be treated as MIMO channels. The model developed in Chapter 3 for frequency selective OFDM and this chapter for MIMO will now be unified to present a MIMO OFDM model.

Consider a MIMO channel with resolvable multipath. Let the transmitted signal be given by

$\mathbf{x} = \begin{bmatrix} x_1 & x_2 & \cdots & x_t \end{bmatrix}^+$, where '+ ' stands for the transpose operation.

Let the received signal be

$$\mathbf{y} = \begin{bmatrix} y_1 & y_2 & \cdots & y_R \end{bmatrix}^+$$

and the noise vector be

$$\boldsymbol{\eta} = \begin{bmatrix} \eta_1 & \eta_2 & \cdots & \eta_R \end{bmatrix}^+$$

The relation between the received signal in antenna *r* and the transmitted signal can be written as

$$y_r(n) = \sum_{t=1}^{T} \sum_{k=0}^{K-1} x_t(n-k) h_{tr}(k) + \eta_r(t)$$

where $x_t(n)$ is the n[th] transmitted symbol from antenna *t*

$y_r(n)$ is the n[th] received symbol at antenna *r*

$h_{tr}(k)$ is the spatially correlated k[th] Raleigh fading tap from antenna *t* to antenna *r*. The maximum number of resolvable taps from antenna *t* to antenna *r* is K.

As done before, assuming the cyclic prefix to be longer then the sum of the last resolved tap and the timing error and perfect timing and frequency synchronization, DFT of the channel taps gives a resultant taps in the frequency domain that are decoupled.

The taps are assumed to be linear, time invariant and Bound Input Bounded Output (BIBO) stable. Hence, superposition can be employed for each set of taps from transmit antenna *t* to receive antenna *r*, resulting in a vector of frequency taps corresponding to each transmit/receive antenna pair. Assuming a 64 point DFT being employed, we get the following expression in the frequency domain:

$$y_r^f = \sum_{t=1}^{T} h_{tr}^f x_t^f + \eta_r^f$$

Here, in order to differentiate between the spatial and frequency domain, following convention is used. The subscript denotes the spatial domain and the superscript the frequency domain.

h_{tr}^{f} corresponds to the channel gain for channel index *f* for a the given transmit/receive antenna pair *t* and *r*. Writing in matrix form,

$$\begin{bmatrix} y_1^f \\ y_2^f \\ \vdots \\ y_R^f \end{bmatrix} = \begin{bmatrix} h_{11}^f & h_{21}^f & \cdots & h_{T1}^f \\ h_{21}^f & h_{22}^f & \cdots & h_{T2}^f \\ \vdots & \vdots & \vdots & \vdots \\ h_{1R}^f & h_{2R}^f & \cdots & h_{TR}^f \end{bmatrix} \begin{bmatrix} x_1^f \\ x_2^f \\ \vdots \\ x_T^f \end{bmatrix} + \begin{bmatrix} \eta_1^f \\ \eta_2^f \\ \vdots \\ \eta_R^f \end{bmatrix}$$

where η_r^f is the noise seen in the sub channel *f* in receiver *r*. As in Chapter 3, it is white in frequency domain with the same $N(0,\sigma^2)$ pdf as in the time domain AWGN at the receiver.

Assuming an 802.11 OFDM DFT depth, there are 64 such equations corresponding to each sub channels. SVD can be carried out on each matrix to get a diagonalized output as before.

By pre multiplying with **V** on the transmit and $\mathbf{U}^h$ on the receive, we obtain the following expression (assuming R = T) for each of the 64 sub channel matrices.

$$\begin{bmatrix} z_1^f \\ z_2^f \\ \vdots \\ z_T^f \end{bmatrix} = \begin{bmatrix} \delta_1^f & 0 & \cdots & 0 \\ 0 & \delta_2^f & \cdots & 0 \\ \vdots & \vdots & \ddots & \vdots \\ 0 & \cdots & 0 & \delta_T^f \end{bmatrix} \begin{bmatrix} x_1^f \\ x_2^f \\ \vdots \\ x_T^f \end{bmatrix} + V \begin{bmatrix} \eta_1^f \\ \eta_2^f \\ \vdots \\ \eta_T^f \end{bmatrix}$$

A equivalent channel model for the transmitter and channel can now be constructed using the above expression. Figure 27 shows equivalent model. Only the 48 data sub channels corresponding to the IEEE 802.11 OFDM scheme are shown but the model can be extended to all the used sub channels.

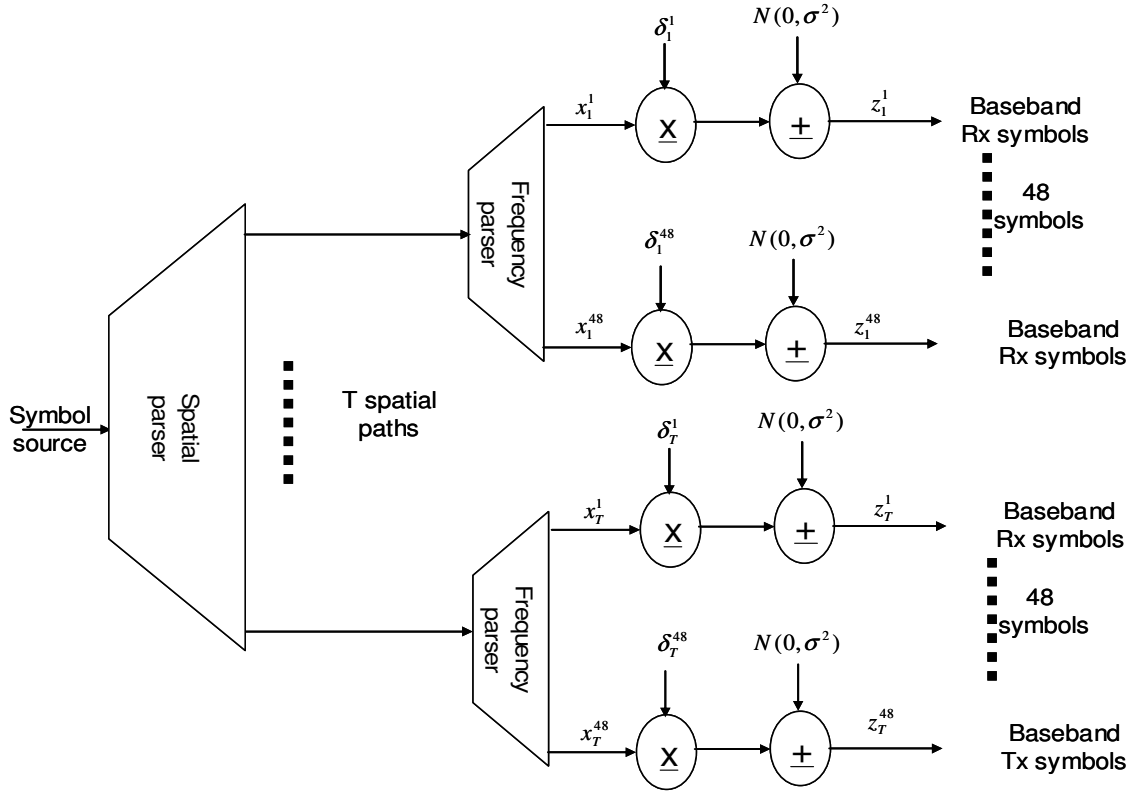

Figure 27: Simple base band equivalent model MIMO OFDM Transmitter and channel using SVD

The receiver is also modeled as a combination of two multiplexers, the first one in the frequency domain and the second one in the spatial domain as shown below.

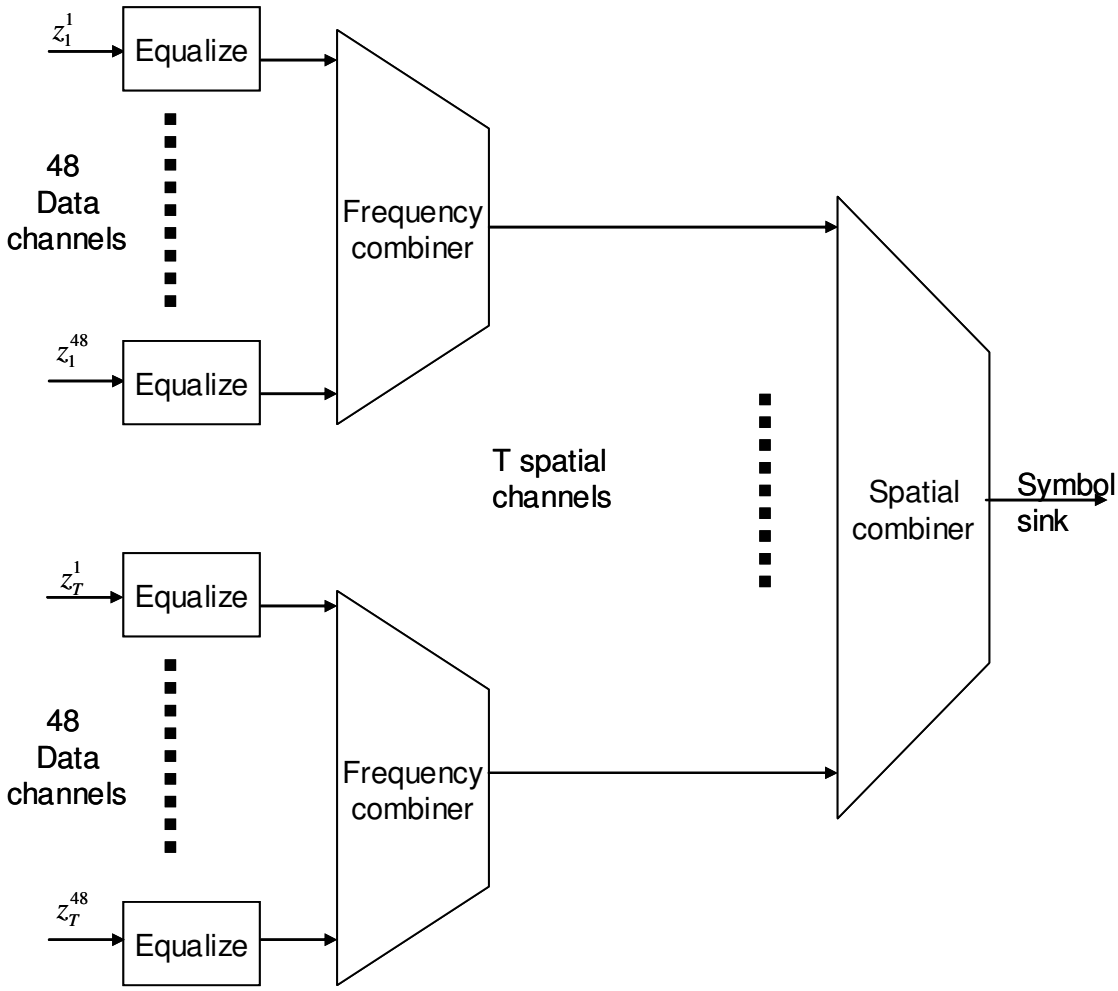

Figure 28: Simple baseband OFDM MIMO receiver model using SVD

4.7 Estimating the coding and modulation type to be used

One way to select the modulation and coding type is to extend the technique discussed in chapter 3 to the case of MIMO channels. In this case, effective SNR can be computed on the full system or per channel basis to get and idea of the modulation type that can be used to find the possible rate. Consider the 4x4 MIMO channel shown in Figure 29. Each curve represents the channel gain in a particular spatial channel and the '*' represents the gain in a particular channel index. Since T = R = 4, the number of spatial channels is 4 in this case.

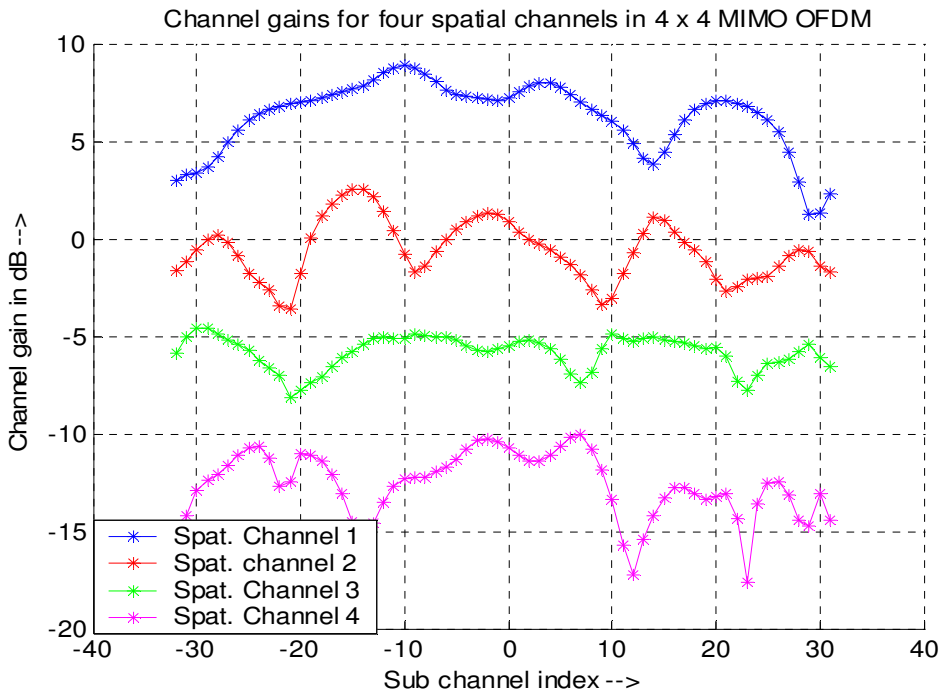

Figure 29: Channel gains for a 4x4 MIMO OFDM system

The bit error rates can be computed for a given modulation type by using the channel gain. Consider the case of BPSK. From chapter 3, bit error probability for a single sub channel is given by the expression

$$P_t^f = Q\left(\left|h_t^f\right| / \sigma\right)$$

where P_t^f is the bit error rate for sub channel f and spatial channel t

h_t^f is the sub channel gain in spatial channel t

σ is the standard deviation in frequency domain from AWGN of $N(0,\sigma^2)$

Assuming T = R, the bit error rate over the system for all the spatial channels is given by

$$P_{ave} = \frac{1}{48}\frac{1}{T}\sum_{t=1}^{T}\sum_{f=1}^{48} Q\left(\left|h_t^f\right| / \sigma\right),$$

T is the number of spatial channels and there are 48 data channels in the 802.11 OFDM. The per spatial bit error rate is given by

$$P_{tave} = \frac{1}{48}\sum_{f=1}^{48} Q\left(\left|h_t^f\right| \Big/ \sigma\right)$$

where t is the spatial channel index. Each spatial channel can be evaluated independently for BER performance

As in the case of MIMO channel without multipath, a spatial channel with weak channel gain can remain unused with minimum impact on the channel capacity. In order to do this, it is essential to compute the equivalent SNR for each spatial channel and comparing it against a threshold value to see if it could be used. The effective SNR can also be used for rate selection. As done in chapter 3, the lookup table based approach can be used to find the effective SNR that gives the same BER as the average BER of the spatial channel.

The OFDM MIMO using SVD technique is demonstrated using the channel shown in Figure 30. The channel is for a 4x4 MIMO system with OFDM. The channel gains for each spatial channel are shown in Figure 30.

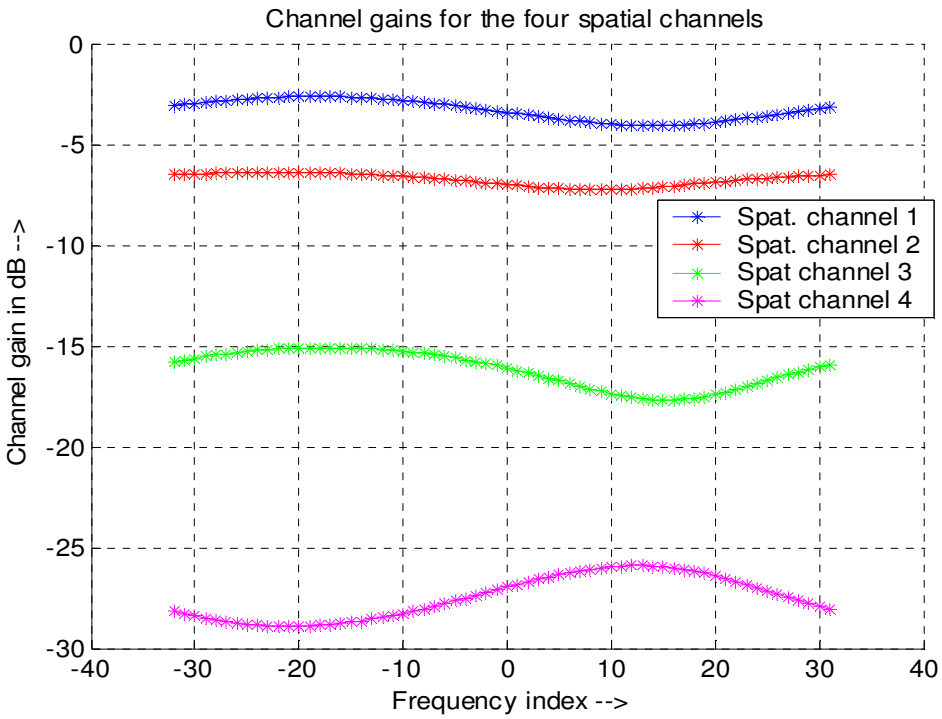

Figure 30: Channel gains for 4x4 MIMO

The simulation was run using million uncoded BPSK modulation. The Figure 31 shows the BER plot on a per channel basis and the combined BER. Spatial channel 1 has the best channel gain and hence the best BER curve. Channel 2 is moderately good while channels 3 and 4 are unusable for the given SNR range. The overall BER is dominated by BER from bad spatial channels.

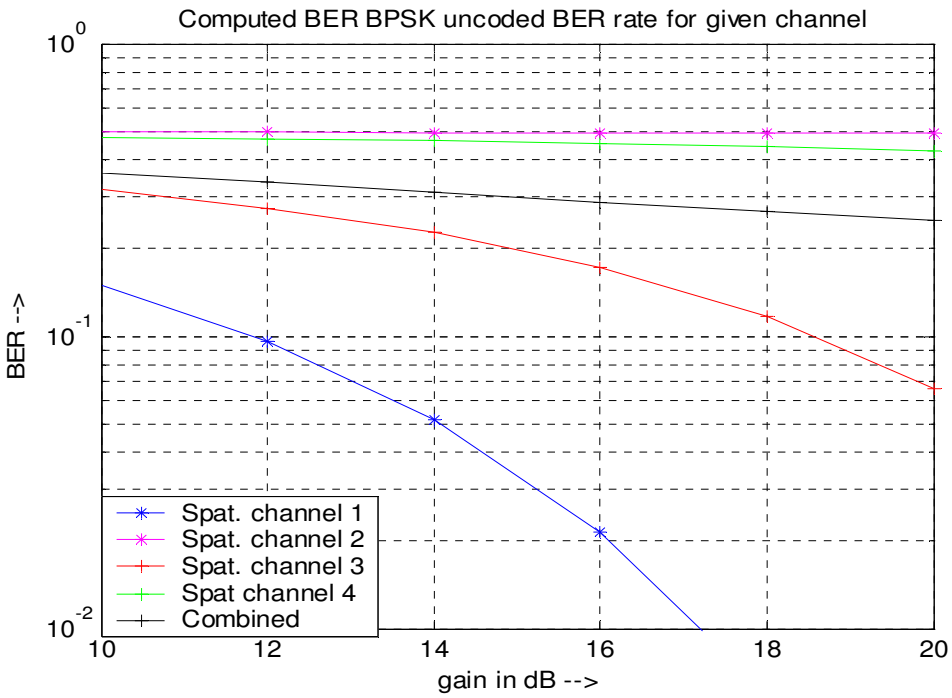

Figure 31: Computed BER for the 4 Spatial Channels in BPSK, uncoded

Figure 32 shows the performance when using rate ½ coding and BPSK modulation. Here, the coding and interleaving was done before the spatial parser. The figure plots the combined BER performance when 1, 2 and 3 out of the 4 spatial channels are used. It is seen that the BER performance degrades as more of the weaker channels are added. It is best with 1 spatial channel, reasonable at high SNR when the best 2 spatial channels are used and gives high BER when 3 spatial channels are used because of the low channel gains and consequent bad BER performance of spatial channel 3. The BER performance if spatial channel 4 was also used can be expected to be worse then the case where spatial channels 1,2 and 3 were used because the BER for spatial channel 4 is the highest.

Using more spatial channels improves the overall throughput. For example, with 1 spatial channel, the raw throughput would be 6 Mbps, with 2 spatial channels would be 12 Mbps and so on. Taking the packet error rate into consideration, assuming a MAC layer that resends corrupted packets, the high BER would bring down the effective throughput drastically. There needs to be a tradeoff between the raw throughput and the packet error rates. Following Chapter 3, we need a BER of 10^{-5} to satisfy the higher layer requirements,

two spatial channels can be used at SNR higher then 20 dB for the given coding and modulation type. Below that, only one spatial channel can be used to obtain the targeted BER.

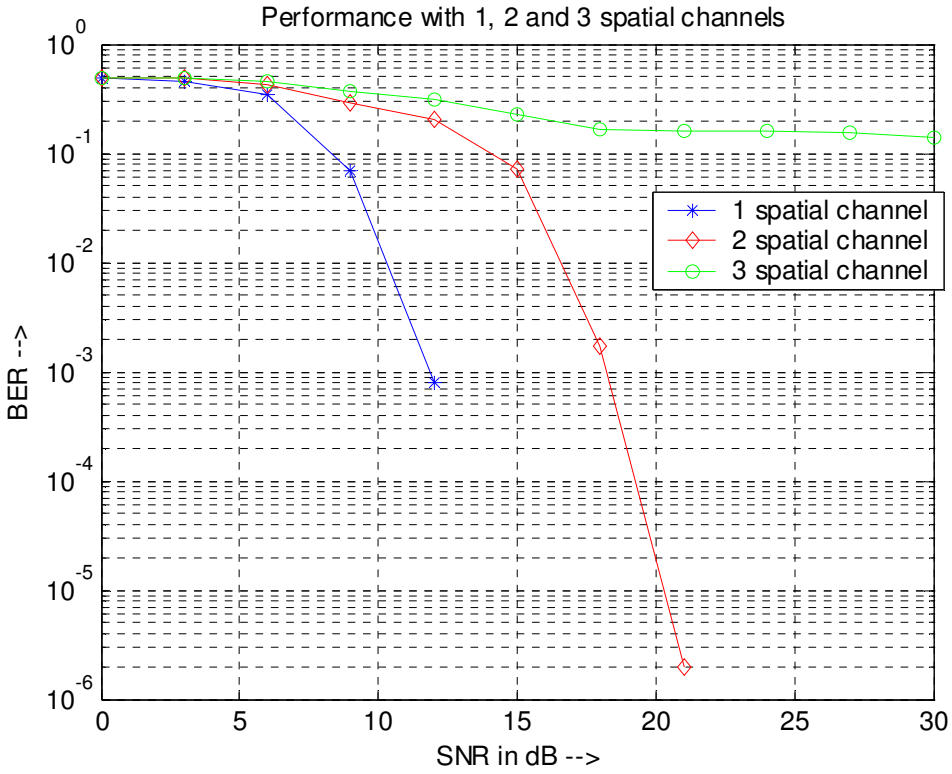

Figure 32: BER plots for BPSK rate ½ using different number of channels

4.8 Summary of Chapter 4

In this chapter, Singular Value Decomposition was used to decompose a flat MIMO channel into parallel spatial channels. The channel gains were used to compute the BER on a per channel basis and the combined BER using all the spatial channels.

The SVD based decomposition was combined with DFT to obtain a parallel channel model in case of frequency selective MIMO channel. Equivalent frequency domain parallel fading channels were used to obtain the spatial sub channel gains.

As discussed in chapter 3, the BER performance of the spatial channel can be deduced by knowing the spatial sub channel gains and by the use of lookup table to find the effective

SNR. The spatial channel gains in the parallel sub channels can be used to compute the per-channel BER from the lookup table and the effective SNR. The effective SNR can then be used along the threshold table (Table 5) to select the rate to be used. The effectiveness of this rate selection approach is shown in Chapter 5.

5 Application and simulation result

Suggested applications of the ideas developed in the previous chapters are discussed in this chapter. The main ideas were the decomposition of MIMO OFDM channel into orthogonal time and frequency domains so that the channels can be viewed as independent and parallel flat fading channels. Also, the expected performance can be judged by the effective SNR. This chapter deals with two possible schemes that take advantage of the MIMO spatial channels in OFDM. The possible gains when operating with legacy single antenna systems are also looked into.

5.1 Simulation setup

All the simulations use 10,000,000 random data bits. The packet sizes are assumed to be 256 bits long. The channel models are based on TGn indoor channel models, which are explained in Appendix 1, but without taking into account Doppler shift and fluorescent light harmonics. The antenna array is assumed to be Uniform Linear Array with $\lambda/2$ separation.

The TGn channel model are divided into 6 distinct models designated by letters A to F. The classification is based on the number of scatters. Channel A is direct line of site with no multipath.

In the simulation, it has been assumed that both the transmitter and the receiver have perfect knowledge of the channel from channel sounding or from the training sequence at the start of the frame.

The actual simulation has two distinct parts. The first part runs on MATLAB and generates the channels using the TGn based channel model generator explained in Appendix 1. It also performs the FFT and SVD on the channels to obtain the channel gains.

The second part runs in C and models the 802.11n system in frequency domain base band. It implements the convolution encoder, Viterbi decoder, interleaver, modulator, demodulator and the parallel channels required to simulate the system. It also computes the equivalent SNR from the SNR/BER table that has been hard coded into the code. The outputs generated such as the code rates selected, number of spatial channels used, BER

and SNR are written into an output file which is used by the MATLAB code to generate the required plots.

5.2 Best Rate Scheme

In Best Rate Scheme, a common modulation and coding is selected for all the usable spatial channels so that the throughput is maximized. If some of the channels cannot support the rate, they are not used. The idea is illustrated in the following example.

Consider a system in which two spatial channels 1 and 2 are possible. Let the spatial channel 1 be the channel with the best channel gain. Using the channel gain based criterion described in chapter 3, suppose the channel 1 has equivalent SNR to support a rate of 9 Mbps and channel 2 has gain to support a rate of 6 Mbps. 6 Mbps can be selected for the overall system because the two spatial channels running 6 Mbps gives a 12 Mbps throughput, which is more then what is possible using channel 1 running 9 Mbps.

On the other hand, if the channel 1 was good enough to sustain 18 Mbps and channel 2 is only good enough for 6 Mbps, it is better to use only channel 1 with 18 Mbps and not channel 2 because it has a throughput greater then the two channels each running 6 Mbps.

Figure 33 describes the transmit architecture for the proposed scheme.

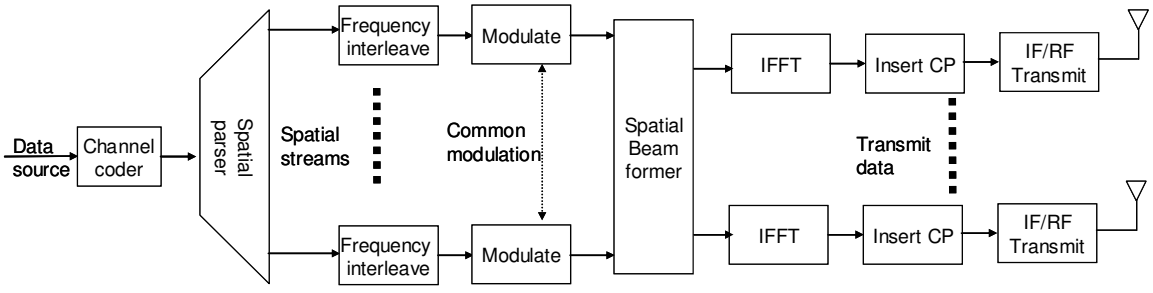

Figure 33: Best Rate Scheme Transmitter Architecture

The transmitter has a common channel coder. The coded bits are split into parallel spatial channels. The bits are interleaved and modulated. The modulation used is same for all the

spatial channels. The spatial symbol streams are multiplied with matrix **V** to get the transmit symbols in the frequency domain. IFFT operation is performed on these symbols to obtain the time domain symbols and cyclic prefix is added as per the 802.11 OFDM specifications to obtain the symbols to be transmitted.

The receiver model is as shown in Figure 34.

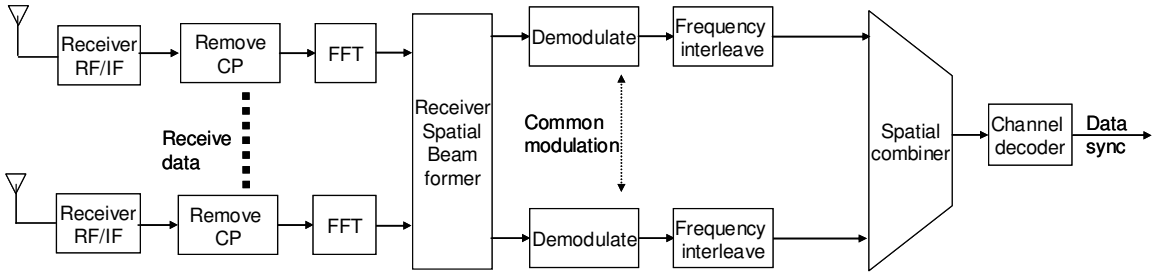

Figure 34: Best Rate Scheme receiver architecture

The receiver is similar to standard 802.11 OFDM receiver, but with multiple receive antennas. The received signals are processed as usual 802.11 OFDM symbols and the frequency domain signals are obtained. The frequency domain signals are then multiplied by the vectors in the **U** matrix to obtain the spatial channels. The spatial combiner then combines the data into a single data stream. The combined stream is demodulated, deinterleaved and decoded to obtain the received data.

As in explained in Chapters 3 and 4, an equivalent frequency domain model was developed to study the performance using simulation. The transmit model in Figure 35. The

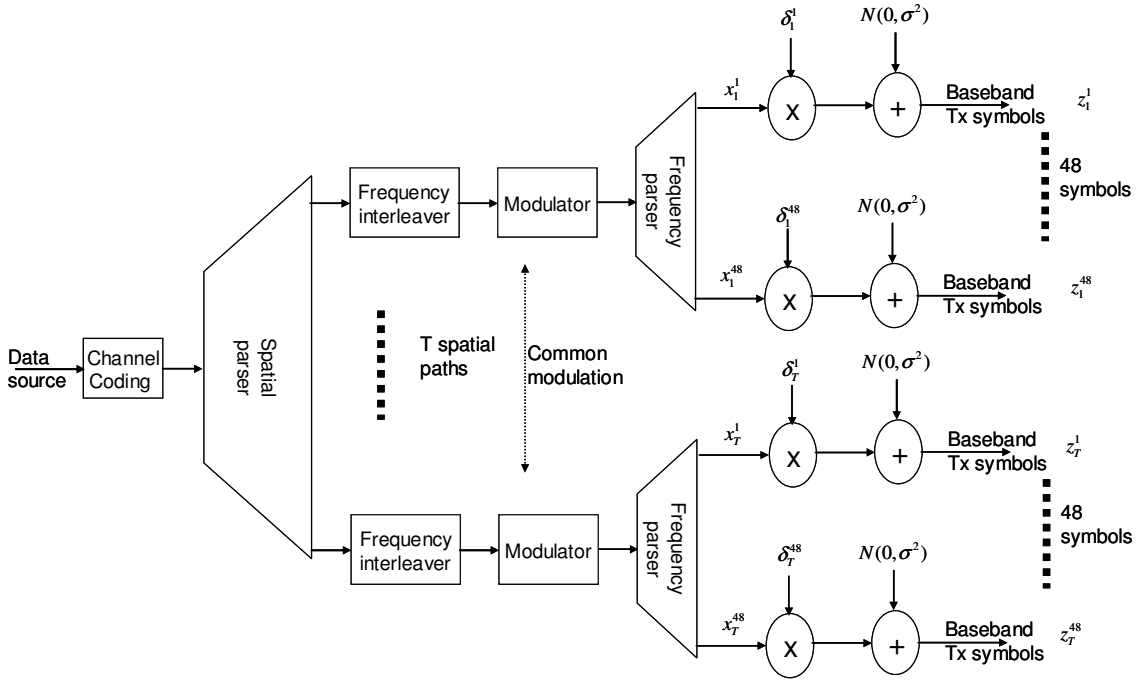

Figure 35: Equivalent base band transmitter and channel model of Best Rate Scheme architecture

In the equivalent model, the channel gains h_t^f represent the gain in sub band *f* and spatial channel *t*. The AWGN noise is added in the frequency domain to get the receive signal.

The receiver is similarly modified to obtain the equivalent frequency domain model for simulation. The equalization is done per sub channel, per spatial channel basis to obtain the received symbol. The symbol is then demodulated, de-interleaved and combined to obtain a single stream. This stream is demodulated to obtain the required output. The equivalent frequency domain model is as shown in the Figure 36

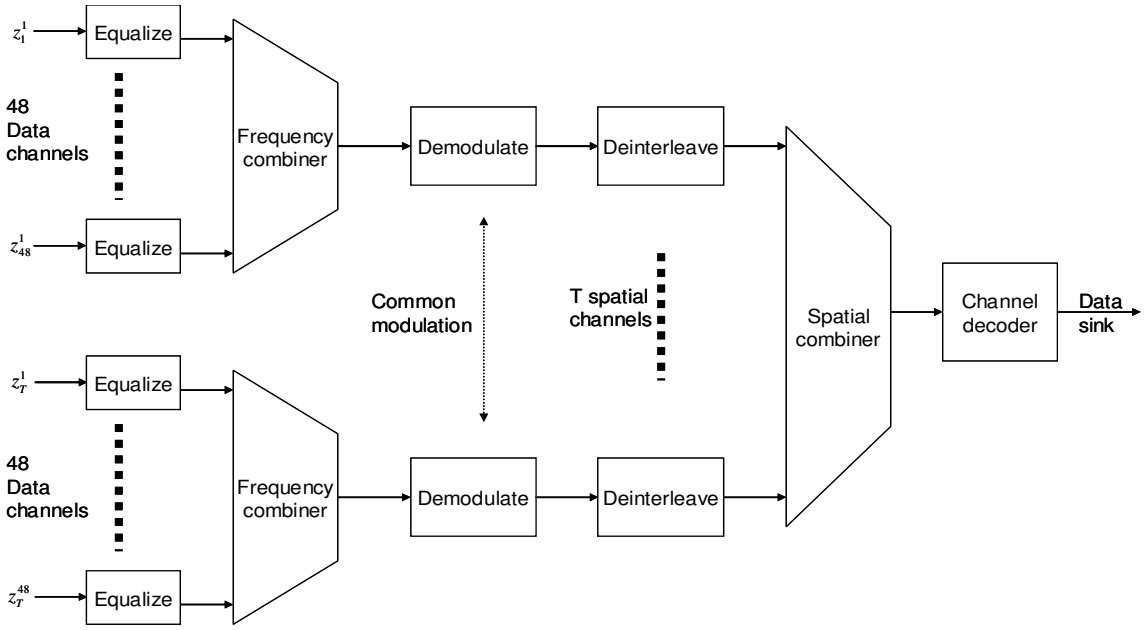

Figure 36: Equivalent Frequency Domain Receiver for Best Rate Scheme

Simulation was carried out using the Best Rate Scheme with two 4x4 channel models based on the TGn channel models.

The first model used was based on TGn channel model B. The channel gains are as shown in Figure 37.

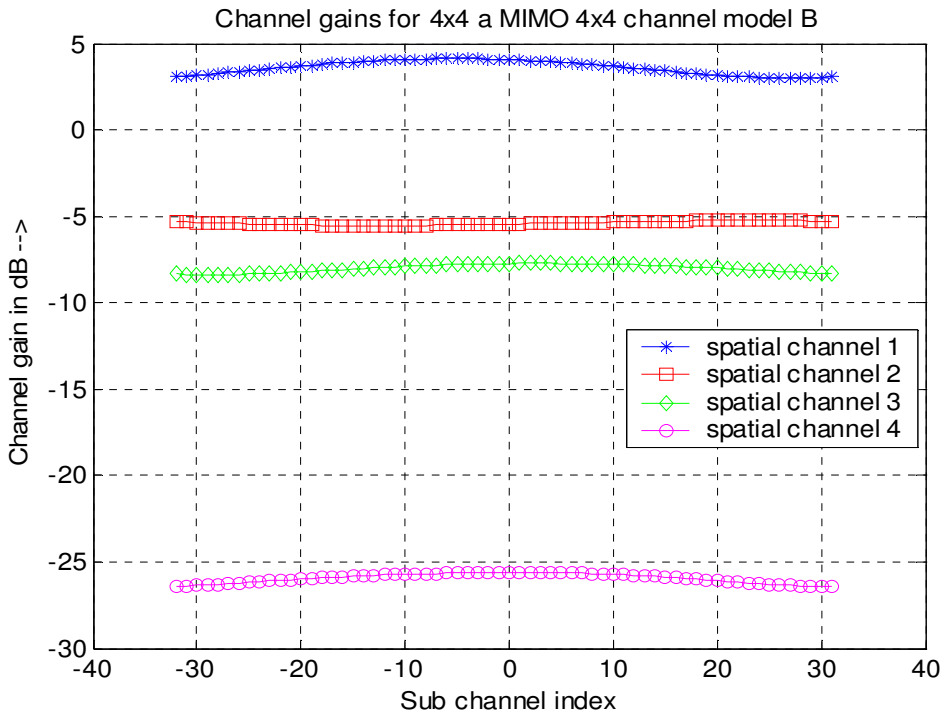

Figure 37: Channel Gain for 4x4 MIMO channel based on model B

BER performance of the system is plotted in Figure 38. It is seen that at many points, the BER is less then 10^{-6}. This is because the effective SNR at that point is well above the threshold of the current rate but below the threshold for the next rate. The throughput rate is plotted in Figure 39. The number of spatial channels used is shown in Figure 40.

It is seen that at SNR of 27 dB, the number of spatial channels used increases from one to two while the per channel throughput falls from 54 Mbps to 36 Mbps to give an aggregate rate of 72 MBps. This is because the effective threshold of the second spatial channel at 27 dB is enough to support a rate of 36 dB and not higher. Spatial channel 1 has good enough effective SNR to operate at 54 Mbps, but since the total throughput rate when both the channels are operating at 36 MBps is higher then channel 1 operating in 54 MBps and channel 2 not being used, 36 MBps rate is selected for both the channels.

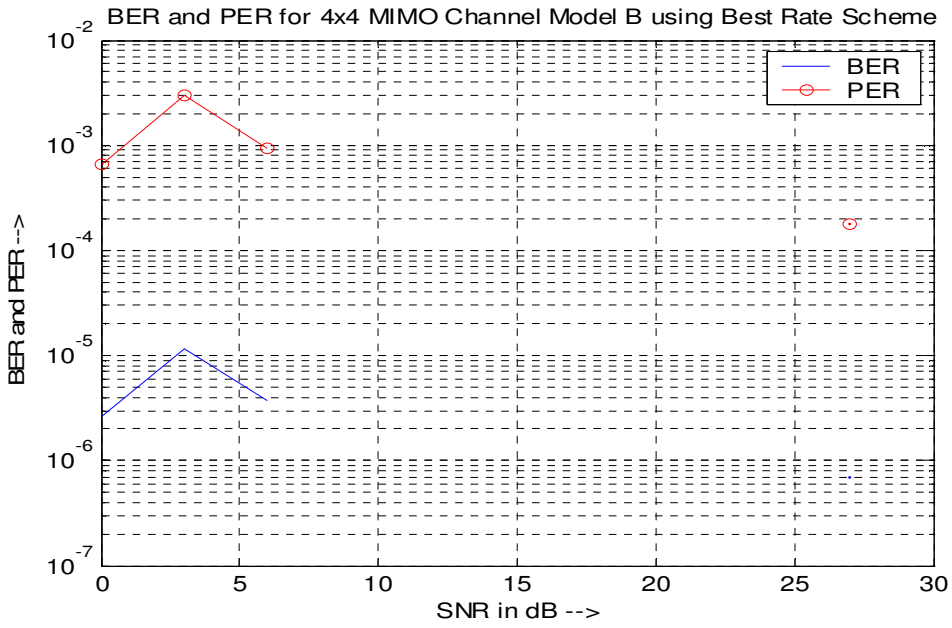

Figure 38: BER and PER performance in MIMO 4x4 Channel model B, using Best Rate Scheme

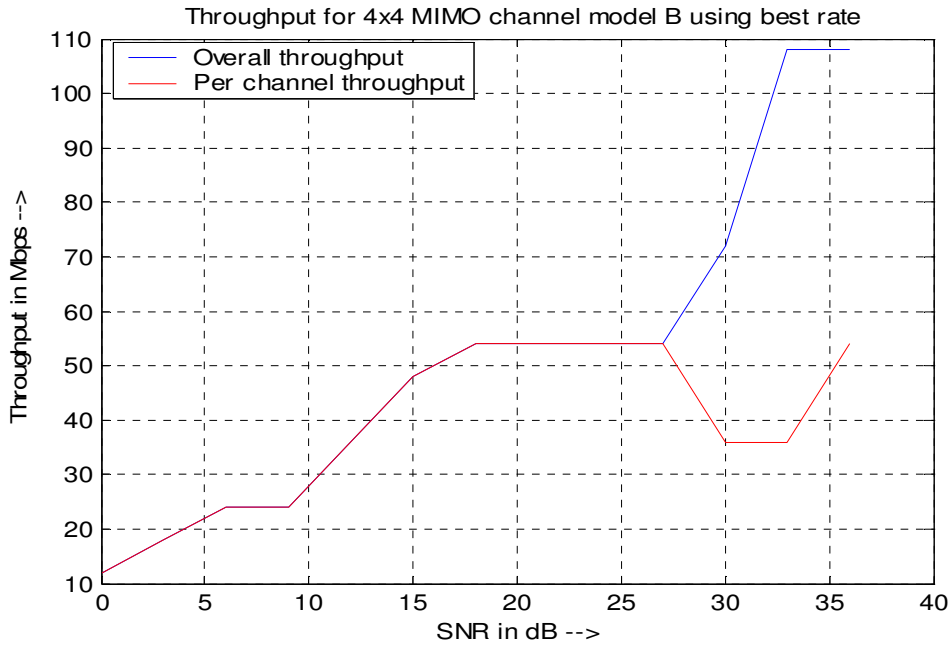

Figure 39: Throughput rate using Best Rate Scheme, 4x4 MIMO channel model B

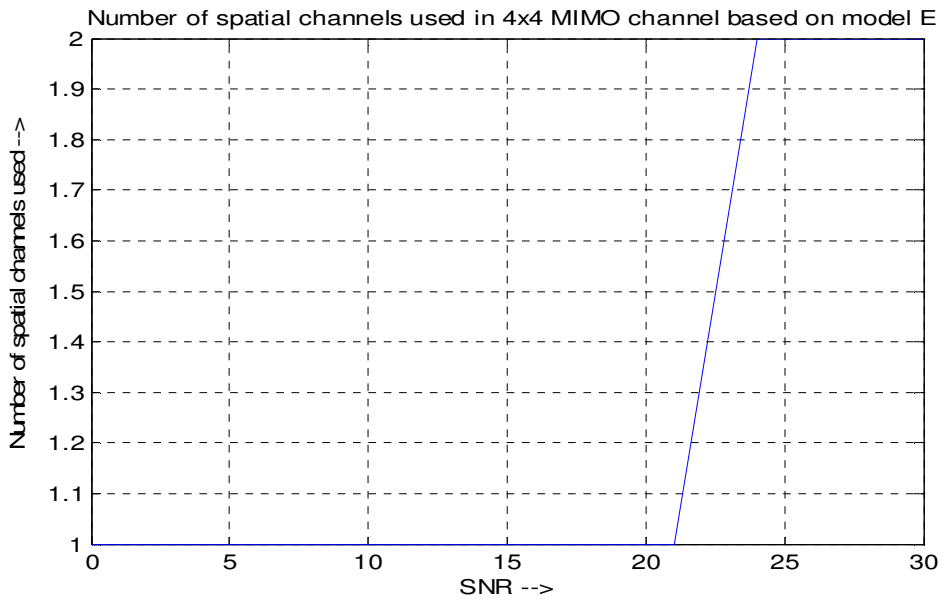

Figure 40: Number of spatial channels used for MIMO 4x4 model B, best rate

The second channel used has a channel model based on TGn model E. The spatial channel gains for different channels are as shown in Figure 41.

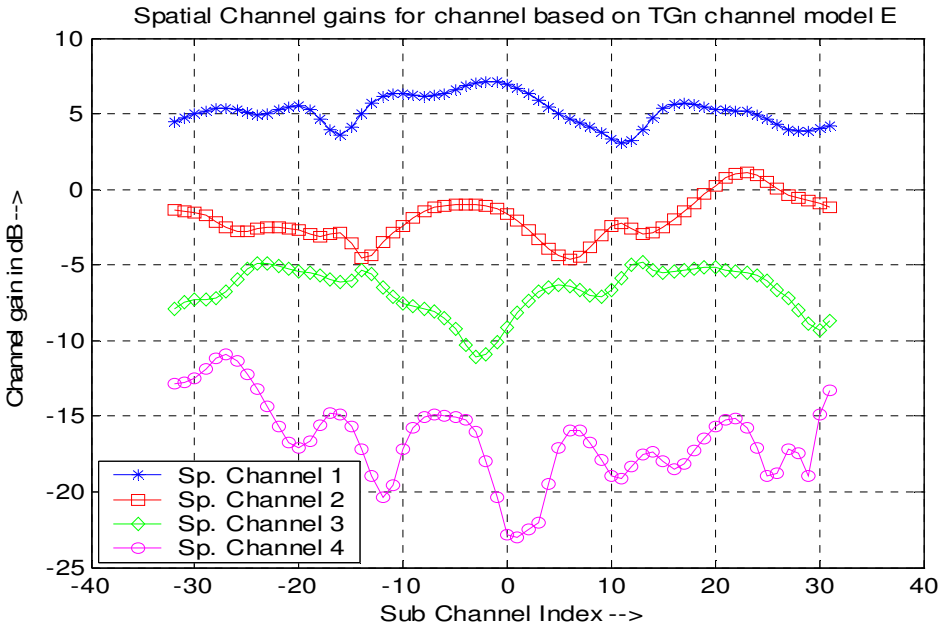

Figure 41: Channel gain for 4x4 MIMO based on Model E

The BER and PER plots are as shown in Figure 42. The points where it is not shown, it is below 10^{-6}.

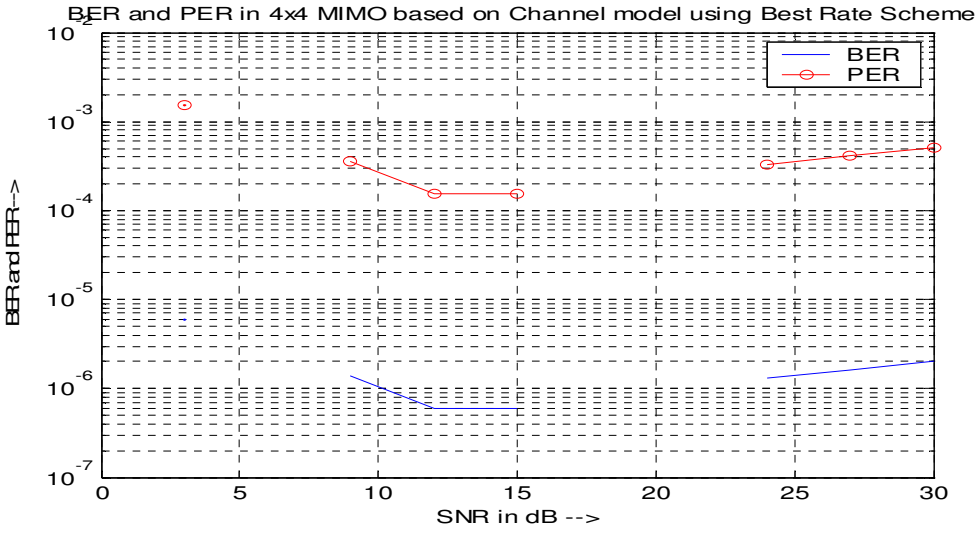

Figure 42: BER and PER plots for the channel model E using Best Rate Scheme

The data rate is shown Figure 42 and the number of spatial channels used in Figure 44

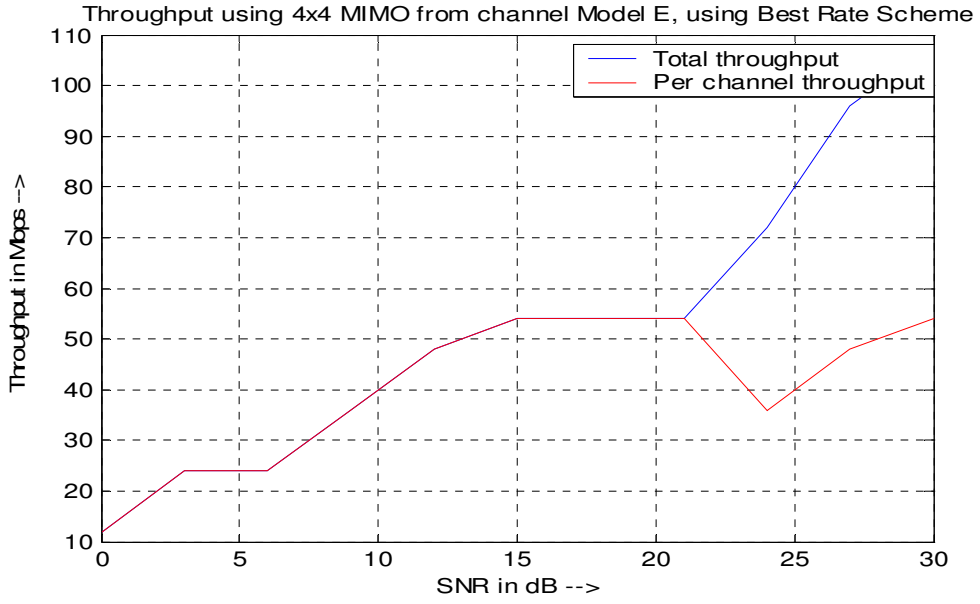

Figure 43: Throughput for Model E channel with Best Rate

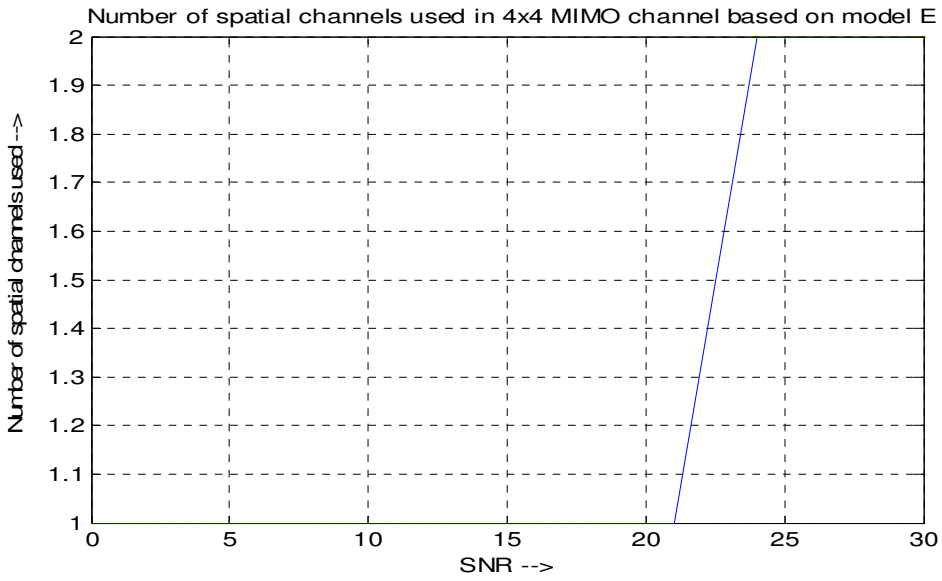

Figure 44: 4x4 MIMO, channel model E Best Rate Scheme Number of spatial channels used

The number of spatial channels used changes from 1 at low SNRs to 2 at 21 dB SNR and above.

The main disadvantage in the above scheme is that it does not optimize the use of the spatial channels. Some of the spatial channels are operated at rates below their highest possible rate. Also, some of the weaker spatial channels cannot be used at all, even though them may be able to handle low data rate. It is however a simple scheme to implement because of the fact that they share a common modulation and coding scheme.

5.3 Bit Loading Scheme for spatial channels

In this scheme, each channel has independent coding and modulation so that the capacity of that channel can be maximized independent of other channels. The channels can be used at their optimum rates independent of other spatial channels and this improves the overall throughput of the system.

The transmitter for Bit Loading Scheme is shown Figure 45 below.

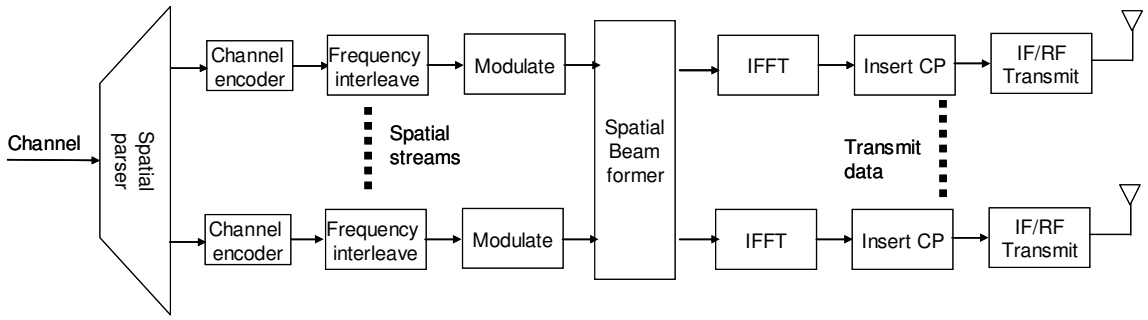

Figure 45: Proposed transmit architecture for Bit Loading Scheme

The transmitter essentially implements the full 802.11a/g transmit side operation is parallel, the only change being the spatial beam former. The receiver complements the transmitter operations in parallel and the data is combined after the decoder. The proposed receiver is shown in Figure 46.

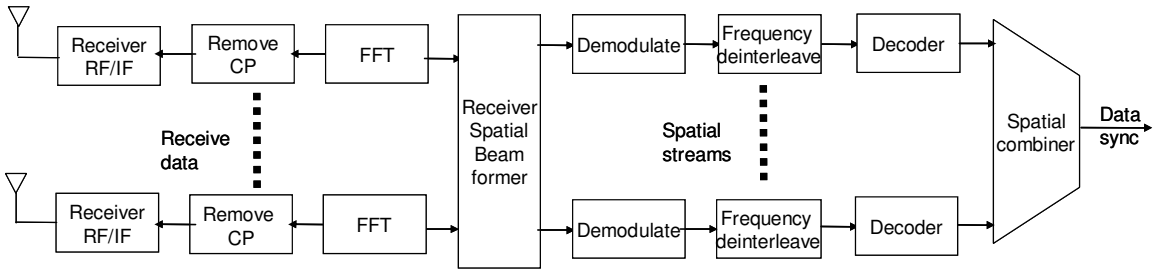

Figure 46: Proposed Receiver Architecture for Bit Loading Scheme

The equivalent frequency domain transmitter and receiver layout is constructed by computing the channel gains in the frequency domain for each spatial channel. The frequency domain equivalents are as shown in Figure 47 and Figure 48.

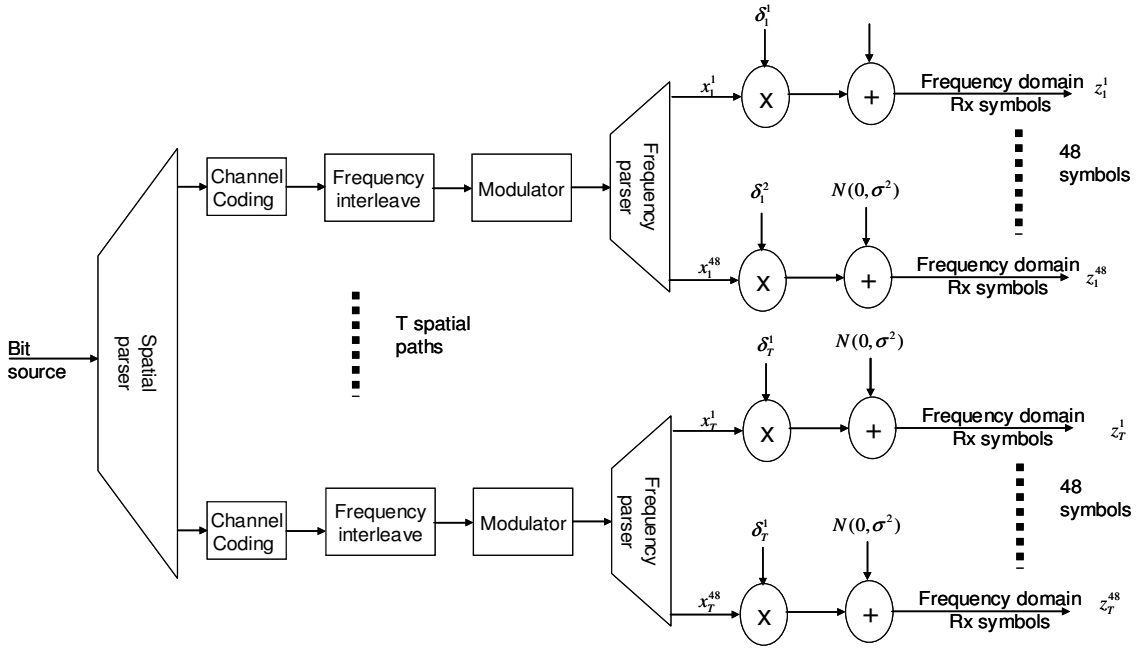

Figure 47: Equivalent frequency domain channel model for Bit Loading Scheme transmitter and channel

The equivalent frequency domain receiver is similar to the Best Rate receiver described before, except the spatial channels are demodulated and decoded independently. It is shown in the Figure 48.

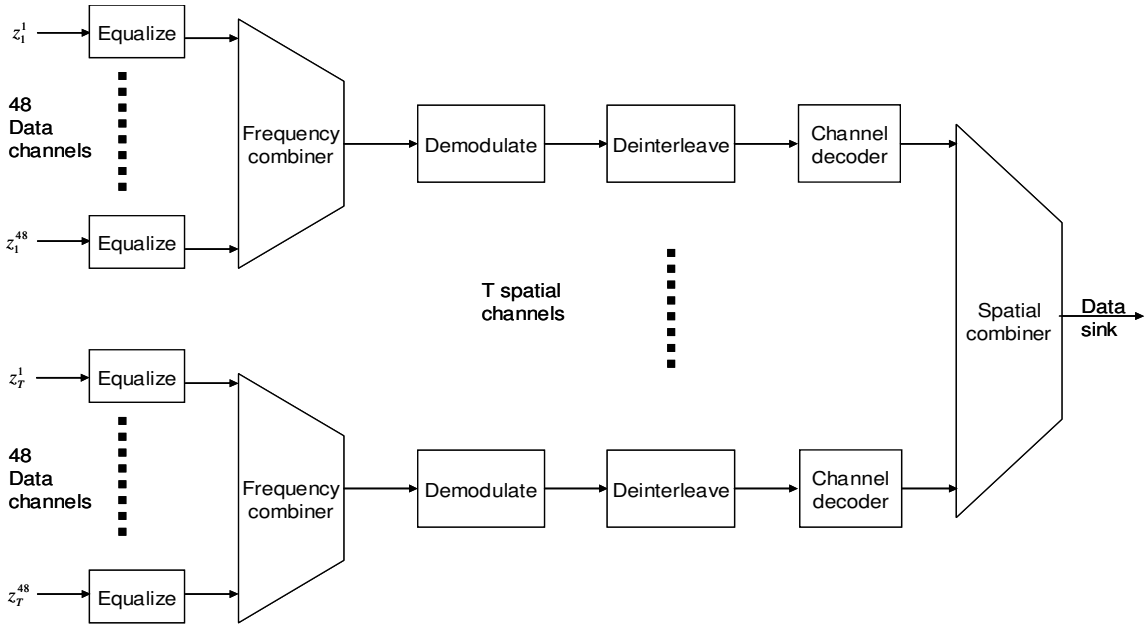

Figure 48: Equivalent frequency domain model for Bit Loading Receiver

The simulated results were obtained for the 4x4 MIMO channels discussed before. The first channel is a 4x4 based on channel model B shown in Figure 37. The BER and PER plots are shown in Figure 49.

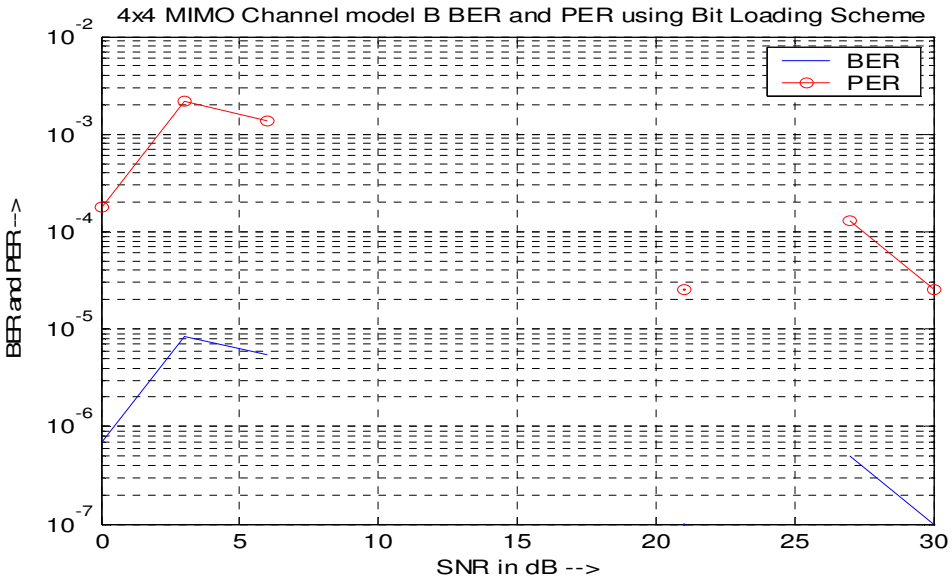

Figure 49: BER and PER plot for channel model B with Bit Loading Scheme

It is seen that the BER is below 10^{-7} for most parts because of the conservative thresholds set up for rate selection.

The data throughput is as shown in Figure 50. It is seen that at high SNRs, there are 3 channels operating ant independent rates, which is more efficient than in the Best Rate Scheme.

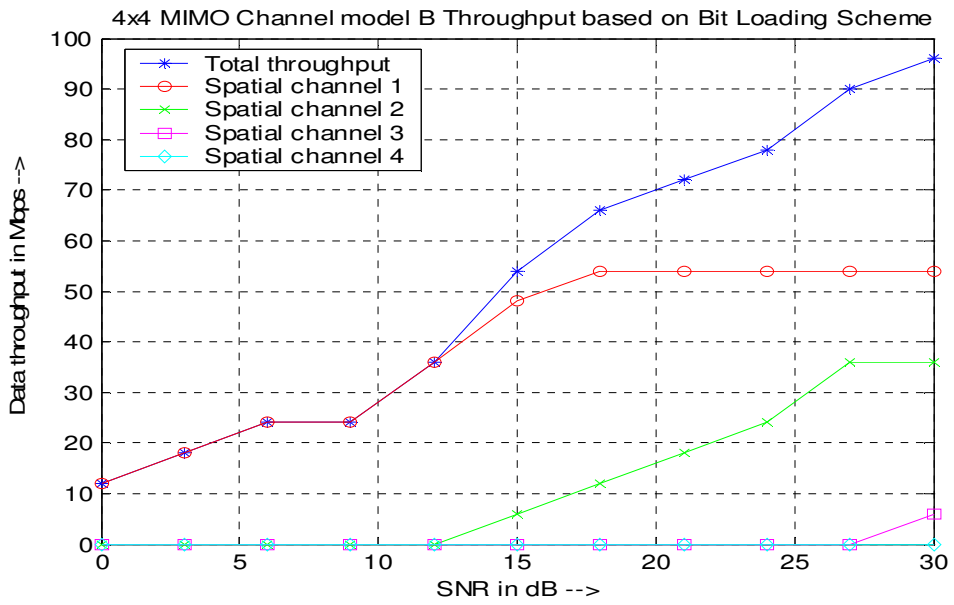

Figure 50: Data throughput with Bit Loading Scheme in channel model B, showing total and per channel throughput

The next set of simulation deals with the 4x4 MIMO based on channel model E shown in Figure 44. Figure 51 gives the BER and PER plots.

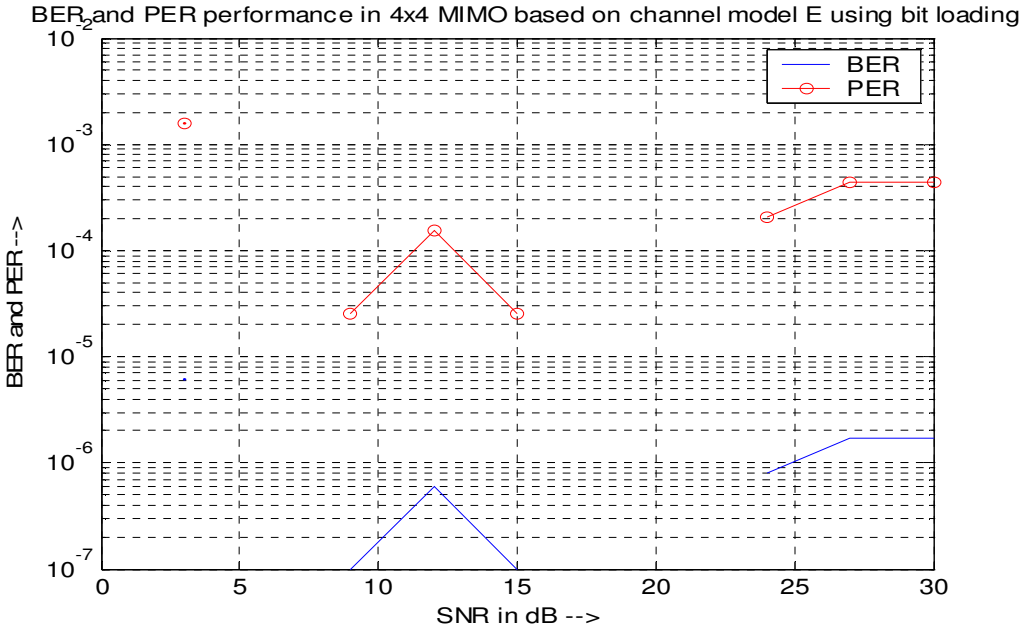

Figure 51: BER and PER plots for channel based on model E with Bit Loading Scheme

The throughput rates are plotted in the Figure 52.

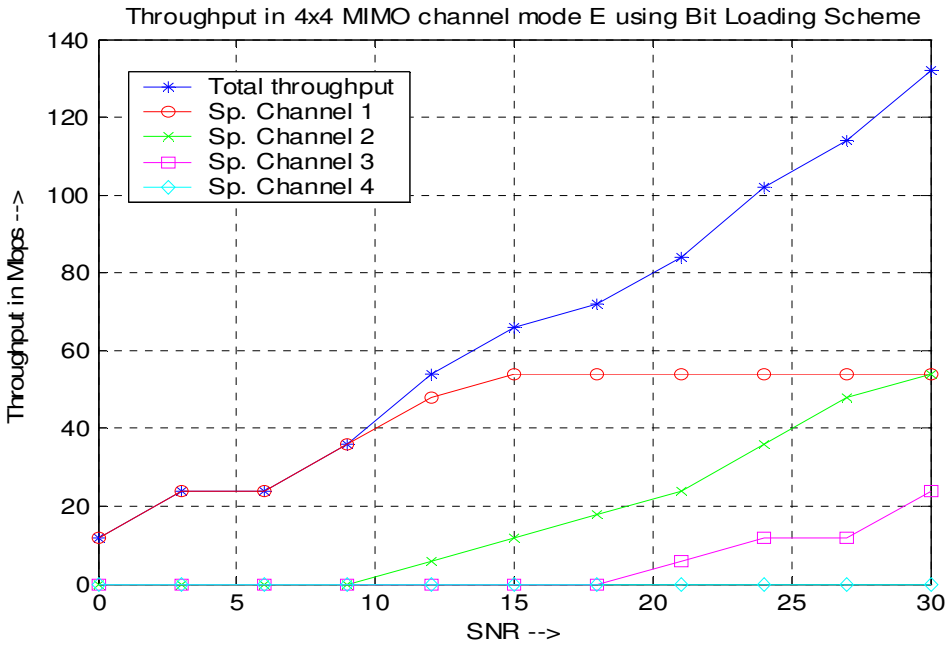

Figure 52: Total and per channel throughput for channel based on model E using Bit Loading Scheme

The Figure 53 compares the performance of Bit Loading and Best Rate Schemes in channel shown Figure 44 with a SISO system with similar channel. It is seen that at a rate of 36 Mbps, a gain of 15 dB is obtained by using MIMO SVD compared to the SISO system. The gains are higher at higher SNR values when more spatial channels come into play.

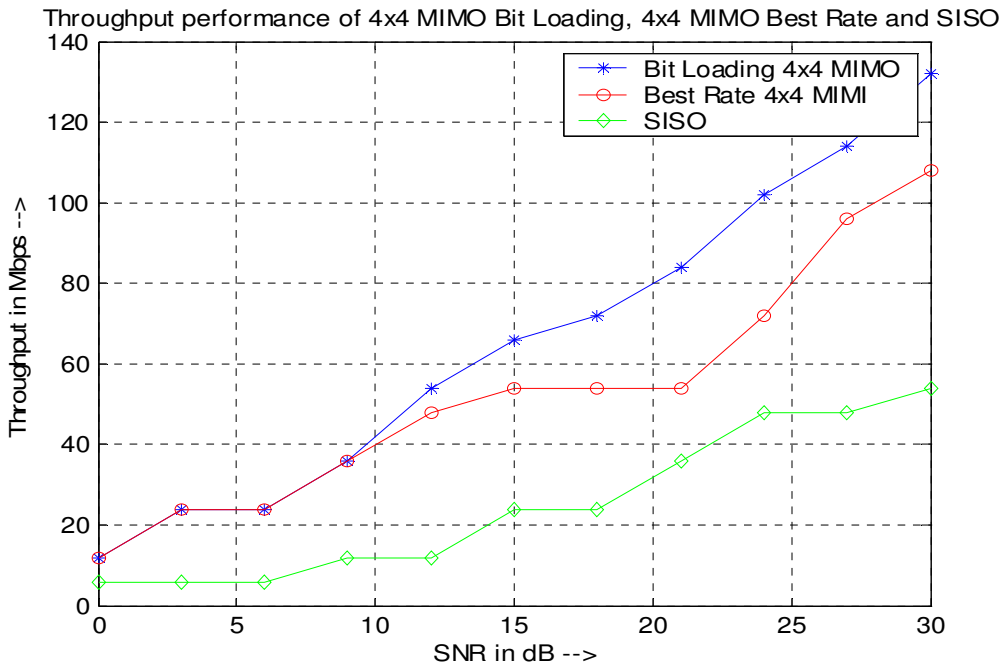

Figure 53: Comparison for throughput rates for 4x4 MIMO with Bit Loading, 4x4 MIMO with Best Rate and SISO

It is seen that the Bit Loading Scheme outperforms the Best Rate Scheme in terms of throughput the higher SNR range when more then one spatial channels come into play.

5.4 Effects of threshold setting on rate selection

The rate threshold for effective SNR can be set to different values depending on the target BER rate. The target BER may be decided by the applications running on the higher layer of the system. For example, a streaming application could have better bit rate error tolerance compared to a bit FTP application. Higher throughput, but with a higher BER can be obtained by setting a lower effective SNR threshold to select a particular rate. In the next simulation, the channel model E shown in Figure 44 is used to compare the throughput performance when the target BER is set to 10^{-3} and when the target BER is set to 10^{-5}. Bit Loading Scheme is used in for comparison.

Figure 54 shows the BER and PER performance using the lower threshold bit filling scheme.

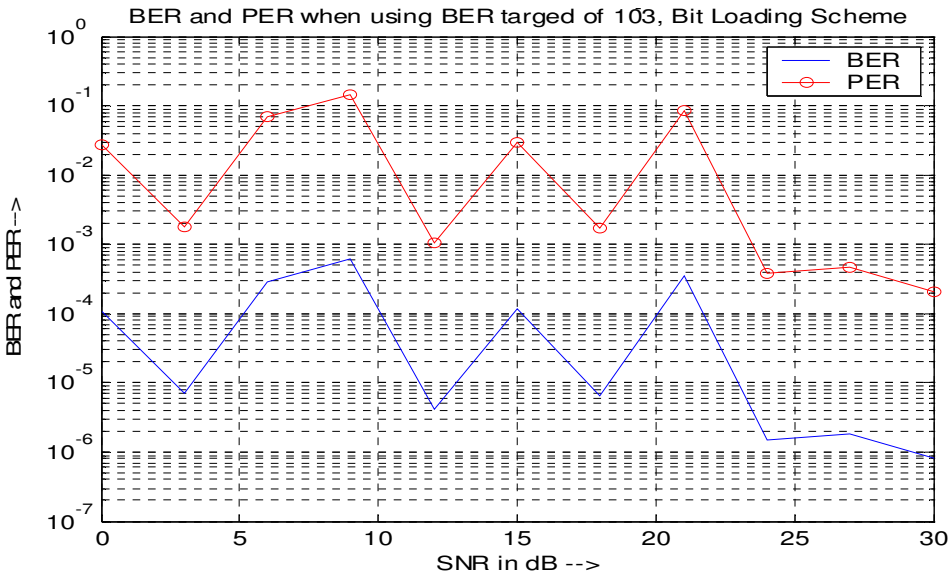

Figure 54: BER and PER plot for bit loading with reduced threshold

Figure 55 compares the throughput rates of lower threshold and higher threshold bit filling scheme.

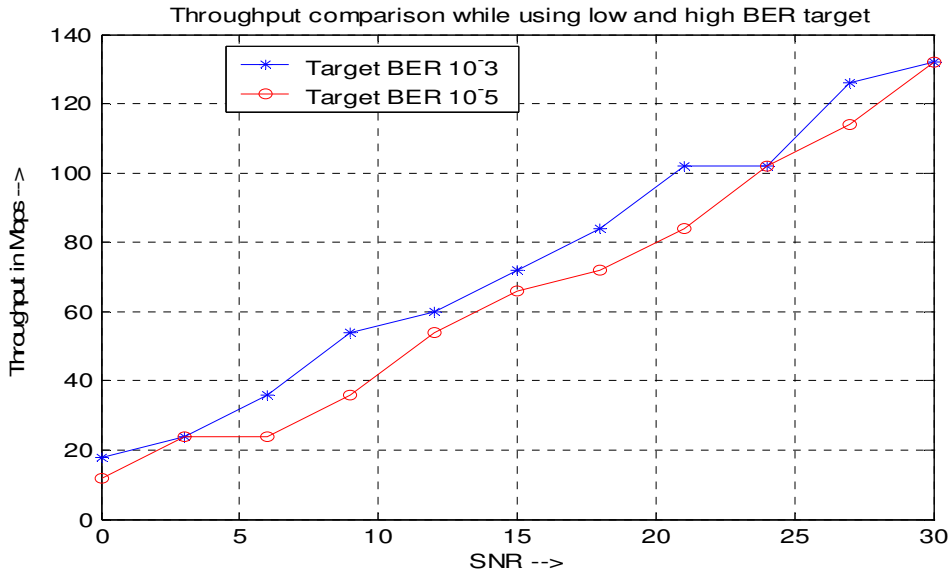

Figure 55: Throughput rate using low and high threshold Bit Loading Schemes

It is seen that at lower SNR values, lower target BER leads to increase in throughput rate at the cost of higher BER rates. A gain of about 3 dB at data rate of 36 Mbps is seen when higher BER is allowed.

5.5 Operation with Legacy 802.11a/g One Antenna Systems

Since backward compatibility with legacy (IEEE 802.11a/g based) systems which have single antenna is required, it would be useful to evaluate the performance in the case where either the transmitter or a receiver is a legacy system and the other uses multiple antennas. It is assumed that since the legacy systems do not respond to the sounding channel, the MAC layer in the proposed 802.11n could assume it is a single antenna legacy system. Also, since the legacy system transmits and receives in a single antenna, there is no need for tone interleaving and the channel model could be found using the long training sequence of the frame. Similarly, when the legacy system is the receiver, the transmit side system does the beam forming. The receiver, in theory, needs to multiply the received signal by a single tap from $\mathbf{U}^h$ in order to equalize. It can be assumed that the receiver could compute the value as in normal equalization.

In the first case, the performance of a four transmit antenna, one receive antenna system is measured against a one transmit, one receive antenna system. It is assumed that the one transmit one receive system follows some rate selection scheme based on channel estimation. The throughputs are compared between the two systems in Figure 56. It is seen that the four Tx one Rx system outperforms the one Tx one Rx system significantly in terms of throughput rate in most of the SNR range tested. The diversity obtained from having multiple transmit antennas help in case where the legacy system is the receiver. The results are plotted in Figure 56.

It is seen that gains up to 7 dB can be obtained at data rate of 36 Mbps by the use of Multiple transmitters and SVD.

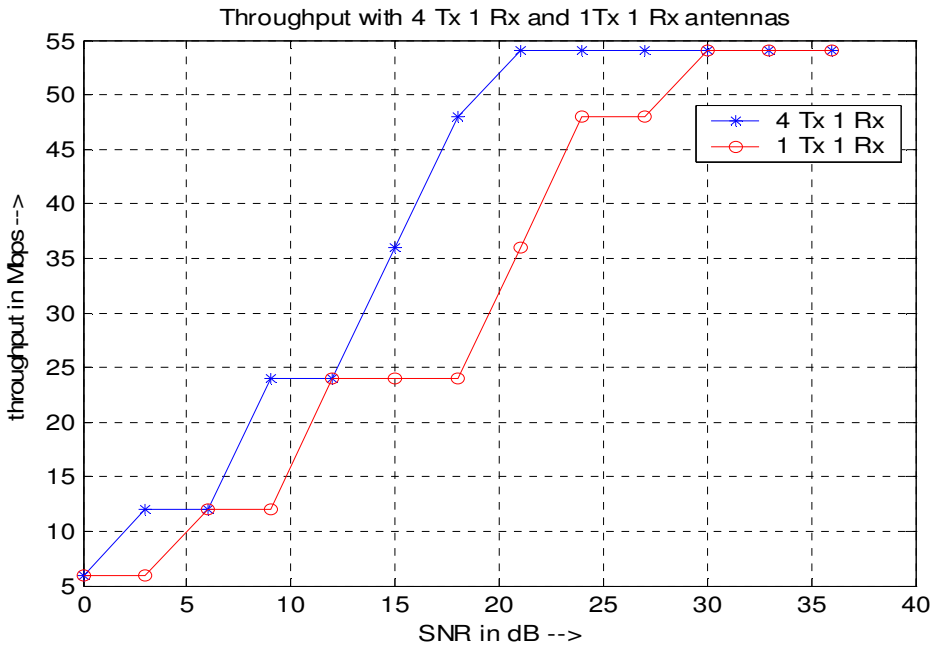

Figure 56: Throughput performance of 4 Tx 1 Rx system and 1 Tx 1 Rx system

In the next simulation, a four receive one transmit antenna system throughput rate is compared with a one transmit one receive system throughput rate. The results are shown in Figure 57

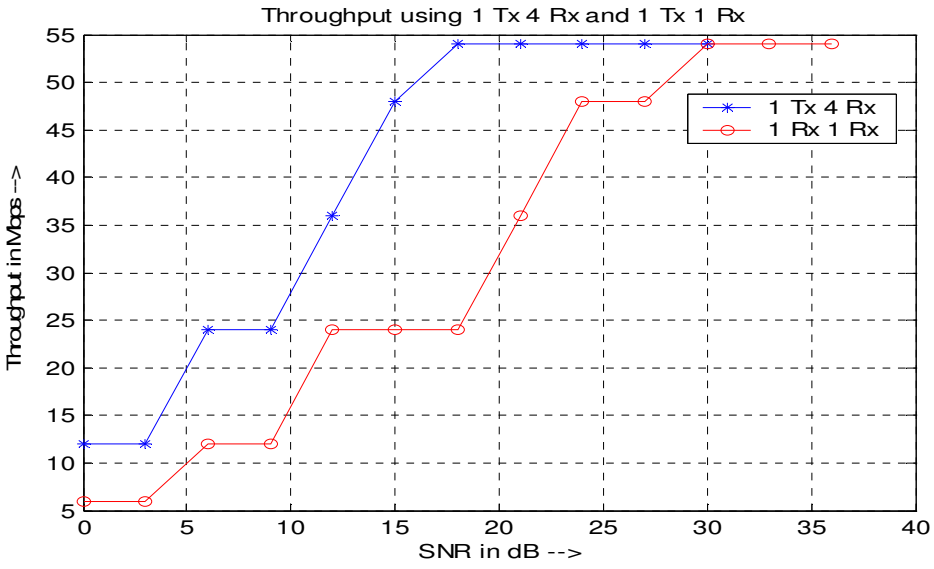

Figure 57: Throughput comparison of 1 Tx 4 Rx system and 1 Tx 1 Rx system

Again, using multiple receivers and SVD, the performance is better then the case of a SISO. At rate 36 Mbps, a gain of around 9 dB is obtained by using multiple receivers and SVD compared to a SISO.

So, even in the case of either the transmitter or the receiver being a legacy system, there is a performance gain in terms of throughput rate when the proposed SVD scheme is used.

6 Conclusion, Implementation Issues and Possible Topics for further research

The thesis suggests a method to select the throughput rate based on the flat fading parallel channel model. The model was developed for a SISO system in Chapter 3 and extended into the MIMO channels by the use of SVD in Chapter 4. The channel gains obtained in the channel model can be used to obtain the effective SNR for the spatial channel based on the SNR-BER table. Using the effective SNR as the threshold, the rate selection can be made. This rate selection strategy was found to be effective in case such as 802.11a/g/n where convolution encoding and interleaving is used.

Chapter 5 demonstrates the use of effective SNR based rate selection scheme for MIMO OFDM.

A very useful property of the algorithm, mainly due to the SVD approach is that it is easy to handle cases where the number of transmit and receive antennas are not the same. An extreme case of this is use of single antenna legacy 802.11a/g systems. The gain in throughput performance when using legacy systems is shown in Chapter 5.

6.1 Some possible constraints and solutions

6.1.1 Channel estimation issues and cycles

A big assumption made in the above method is that the channel is reciprocal and hence the same channel estimation done at the receiver can be used for the transmitter. While this is a valid assumption for the channel per se, the problem comes when the transmit and receive chain hardware are included. The transmit chain of the system that is sending the sounding signals may have High Power Amplifiers (HPAs) that are non linear in frequency domain and the power range. Also, the receiver Low Noise Amplifiers (LNAs) may introduce additional distortions in the device that is receiving the sounding signals. These come into play in the channel estimation since factoring out transmit and receive hardware effects is difficult. In the normal transmission mode, complementary pair of HPAs and LNAs come into picture and they will not have the same spectral characteristics as the one used in sounding. Thus, the gains in rate and BER performance may not be as good as expected. Also, the AWGN is assumed to be the same in both the receivers and this is not true.

Another issue is that SVD is computationally intensive. It is seen that in an 802.11n TGn Sync proposal, the number of SVDs to be done goes up by a factor 64 times the number of spatial channels. But since they are a part of the proposed standard, the IEEE members involved have taken these factors into account. Once SVD is done, the additional computation required to compute the best possible rate is small and can be easily implemented.

6.1.2 Channel estimation in case of non unity transmit power

Another possible implication is the requirement that the transmit side power per sub channel should be known before hand. In the preceding analysis, it was arbitrarily set to unity, which need not be the case. A way to do this would be to have the user terminal transmit the sounding data at a known power level so that the channel gains can be separated from the transmitted power.

Another approach is to have the transmit power information as a part of the sounding packet so that the receiver can do a good estimate of the channel.

6.2 Changes required in the higher layer

The higher layer may need to inform the physical layer in some way as to what is the bit error rate that it can sustain. Also, some form of feed back in form of BER or packet error rate from the receiver could be included so that the transmitter can fall back to a lower rate transmission scheme in case of unexpected problems in the receiver.

6.3 Possible future research areas

6.3.1 Channel model changes

The channel model used here was based on TGn channel model with no Doppler shift. While the Doppler shift in pure indoor environment is negligible, it may not be so in stationary outdoor applications. The channel gains would change in a per frame or symbol basis. Efficient computation of channel gain changes in an incremental way would be a good approach to handle this issue.

Also, the channel model used in the simulation is based on a Uniform Linear Array (ULA). Extending the channel model to include other array configurations would provide more data points to support the research.

6.4 Possible application of this research

The direct application of the research is in MIMO OFDM as discussed earlier. The above research can be extended to include higher layer performance. Also, the performance in presence of interference can be looked into.

The rate selection approach described here can also be used in case of transmit side eigen value based beam forming.

Another idea not explored is linking the BER performance to rate selection. If the BER performance for a particular channel and rate is found to be good (say from feedback), in the subsequent frames, the rate can be moved higher by scaling down the table value by a small delta. Similarly, if the BER performance was below expectation, the table of threshold values can be revised upwards by a small value delta.

6.4.1 Distributed MIMO and Ad-Hoc networks

A possible application of this research is in the field of distributed MIMO. Here, each transmitter/receiver combination can be thought of a single spatial channel and the analysis carried in chapter 3 can be applied to find the data rate possible from each possible pair.

An interesting extension of the scheme would be in case of ad-hoc networks. The channel estimation suggested in chapter 3 and 4 could be used to determine the suitability of a particular path. The effective SNR could be taken as a cost function. The nodes could then use Dijkstra's algorithm [5] to build a best route map to each of the other nodes based on this cost function.

7 Appendix

7.1 Appendix 1: The TGn channel model

The TGn channel model was proposed in the 802.11n the 802.11n working group and is based on the earlier work of (SISO) WLAN channel models proposed by Medbo et al. The main SISO channel model was extended to the MIMO channel model by the adding correlation between antennas based on the antenna configuration and angle of arrival (AOA) or departure (AOD).

Consider a MIMO system where the transmitter is far enough from the receiver so that the angle difference between the received angles is small. Let antenna array be Uniform Linear Array (ULA) with distance d between elements as shown below.

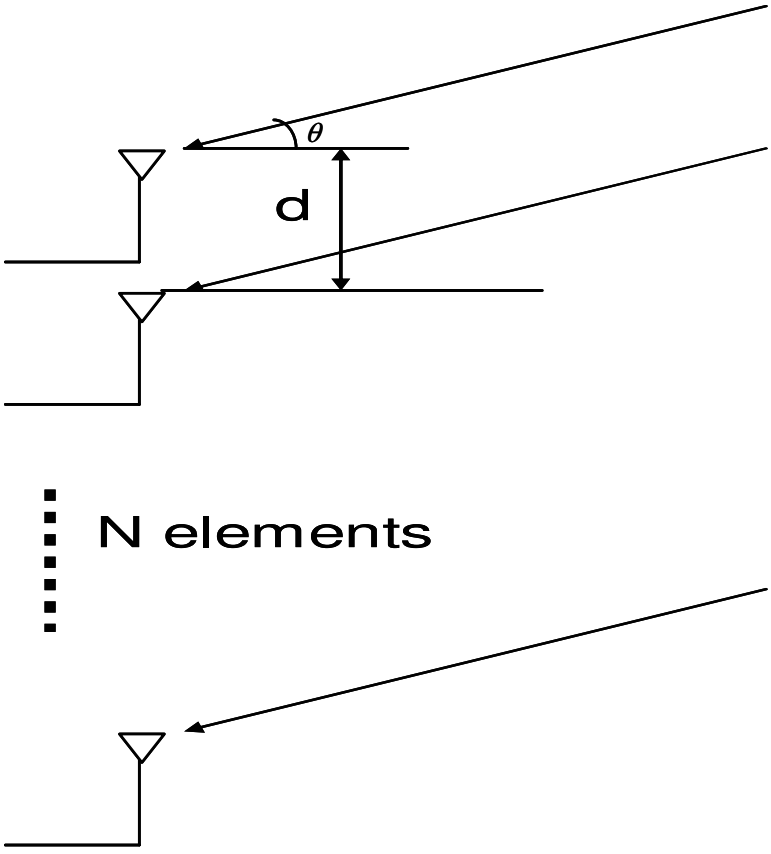

Figure 58: ULA receiver array

The correlation between the received signal in antenna element 1 and element 2 is given by

$e^{\left(j\frac{d}{\lambda}\sin\theta\right)}$, where d is the distance between the 2 antennas and λ is the wave length of the received signal. A common way of expressing the relation is $e^{(jD\sin\theta)}$, where D = $\frac{d}{\lambda}$.

The same relationship holds good for correlation between transmit antennas based on angle of departure.

In case of MIMO channel, the above correlation can be expressed in a matrix form given by

$$\mathbf{R}_{tx} = \begin{bmatrix} 1 & e^{(jD\sin\theta)} & e^{(j2D\sin\theta)} & \cdots \\ e^{(-jD\sin\theta)} & 1 & e^{(jD\sin\theta)} & \cdots \\ e^{(-j2D\sin\theta)} & e^{(-jD\sin\theta)} & \ddots & \\ \vdots & \vdots & & 1 \end{bmatrix}$$

Thus, in case of MIMO channel with Angle of Departure (AoD) of θ_1 and Angle of Arrival (AoA) θ_2 and some independent flat fading F can be expressed as follows:

$$\mathbf{R}_{tx} = \begin{bmatrix} 1 & e^{(jD\sin\theta_1)} & e^{(j2D\sin\theta_1)} & \cdots \\ e^{(-jD\sin\theta_1)} & 1 & e^{(jD\sin\theta_1)} & \cdots \\ e^{(-j2D\sin\theta_1)} & e^{(-jD\sin\theta_1)} & \ddots & \\ \vdots & \vdots & & 1 \end{bmatrix}$$

$$\mathbf{R}_{rx} = \begin{bmatrix} 1 & e^{(jD\sin\theta_2)} & e^{(j2D\sin\theta_2)} & \cdots \\ e^{(-jD\sin\theta_2)} & 1 & e^{(jD\sin\theta_2)} & \cdots \\ e^{(-j2D\sin\theta 2)} & e^{(-jD\sin\theta_2)} & \ddots & \\ \vdots & \vdots & & 1 \end{bmatrix}$$

The channel coefficients between transmit and receive antennas can be generated independently for each tap taking into consideration factors such as distance, shadowing and fading. The fading matrix is assumed to be independent between each transmit-receive

antenna pair and is represented by the matrix $\mathbf{H}_{iid}$. The channel matrix $\mathbf{H}$ for the given tap is then given by

$$\mathbf{H} = \mathbf{R}_{rx}^{\frac{1}{2}} \mathbf{H}_{iid} \mathbf{R}_{tx}^{\frac{1}{2}}$$

The operation $\mathbf{R}_{tx}^{\frac{1}{2}}$ is equivalent to Choleski decomposition of the matrix R_{tx}.

7.1.1 Clustered scatarers

In indoor environments, there are additional non line of sight elements that come from reflection from objects or people. Extensive measurements in indoor situations have indicated that the scaterers are usually bunched together, leading to development of clustered scatterer channel models. In this case, the rays reflected from a particular scaterer have a mean angle of arrival or departure and a finite Angle Spread (AS). The AoA and AoD also have a particular Power Angular Spectrum (PAS) that gives the distribution of the angles around the mean.

The best fit PAS function has been found to be Laplacian function given by the equation

$$p(\theta) = \frac{1}{\sqrt{2}\sigma} e^{-\left|\sqrt{2}\theta/\sigma\right|}$$

Where σ is the AS.

The Correlation function is modified as follows

$$R_{XX}(D) = \int_{-\pi}^{\pi} e^{(jD\sin\phi)} PAS(\phi) d\phi$$

This integration is a Bessel function of first kind. A simple approximation suggested in [14] is used to do the actual computation.

Once the correlation matrix for the transmit and receive antennas are obtained after knowing the cluster AS, mean AOA/AOD and the PAS, Choleski decomposition is carried out and the result multiplied in to obtain the channel matrix for a particular tap. The channel table for different channel models is given in the TGn model document.

7.1.2 Channel generation

TGn channel models are of 6 types and are designated by the letters A to E. Channel model A is direct line of sight with no multipath and is used only as a reference.

The channels are classified by the number of scaterrers and the number of taps they generate.

The channel taps are generated as using the channel model table given in the channel model document. It was assumed that there was no pulse shaping used and hence, all the channel taps that fall between a given 50 nano second sub symbol duration interval were summed together as one effective tap. The steps used were as follows

1. Find all the channel taps with time of arrival between a given sub symbol interval
2. Pick channel taps from random complex Gaussian fading envelope. Scale them according to the expected tap power.
3. Use the cluster AoA, AoD and AS to determine the transmit and receive correlation matrix as described in the section above.
4. Compute the correlated matrix for each tap for a given sub symbol interval.
5. Add all the tap matrix to obtain the channel tap for a given sub symbol interval. Scale the taps based on the shadowing constant using the distance between the transmitter and the receiver
6. To compute the line of sight component, assume the AoA and AoD to be $\pi/4$. Compute the channel matrix with some random complex Gaussian envelope with unity variance. The path loss parameter is assumed to be 1 dB per meter.

7.2 Appendix 2: Singular Value Decomposition

Singular value decomposition is a technique used to decompose non singular, non square matrix into a product of a diagonal matrix and unitary matrices so that a matrix **H** can be written as

$$\mathbf{H} = \mathbf{U}\sum\mathbf{V}^h$$

There exists a strong relationship between the SVD and eigen value decomposition of $\mathbf{HH}^h$

$$\mathbf{HH}^h = (\mathbf{U}\sum\mathbf{V}^h)(\mathbf{U}\sum\mathbf{V}^h)^h$$
$$= (\mathbf{U}\sum\mathbf{V}^h)(\mathbf{V}\sum{}^h\mathbf{U}^h)$$
$$= (\mathbf{U}\left|\sum\right|^2\mathbf{U}^h)$$

Since $\mathbf{HH}^h$ is a hermetian, the eigen values of $\mathbf{HH}^h$ are positive and real. $\sum$ is the square root of the eigen values of $\mathbf{HH}^h$. **U** is the eigen vector matrix of $\mathbf{HH}^h$.

To find **V**, the following relation can be used

$$\mathbf{H} = \mathbf{U}\sum\mathbf{V}^h$$
$$\Rightarrow \mathbf{V} = \sum{}^{-1}\mathbf{U}^{-1}\mathbf{H}$$

Since **U** is a unitary matrix, $\mathbf{U}^{-1}$ is $\mathbf{U}^h$. Also, $\sum$ is a diagonal matrix and the inverse is the same as the inverse of the diagonal element and **V** can be easily computed.

The ratio of the largest to the smallest diagonal values of $\sum$ is called the condition number of the matrix. Greater the condition number, closer the matrix is to being singular.

There are number of numerical methods to compute the eigen vectors and eigen values of a given matrix. The most common method for hermitian matrix is power method, that finds eigen values in a recursive way, the largest one first, and also the corresponding eigen vector. The method has the added advantage that if due to cycle limitations, it is decided that only one or two spatial channels that have the highest spatial gains are to be used, the power method always picks the one or two that give the largest eigen values.

8 References

8.1.1 Text books

[1] John G. Proakis, “Digital Communications”, Fourth Edition, McGraw Hill publishers, 1996

[2] Juha Heiskala and John Terry, “OFDM Wireless LANs: A Theoretical and Practical Guide”, SAMS 2001, 2001

[3] Stephen B. Wicker, “Error Control Coding”, Pretence Hall publishers, 1995

[4] Gilbert Strang, “Linear Algebra and it's applications” Thomson Brook, 1988

[5] T.H. Cormen et al, “Introduction to Algorithms” Chapter 25, McGraw Hill, 1990

8.1.2 IEEE Specifications and proposed specifications

[6] TGn Channel Models

[7] IEEE Std. 802.11a-1999 Part 11: Wireless LAN Medium Access Control (MAC) and Physical Layer (PHY) specifications: High-speed Physical Layer in the 5 GHZ Band

[8] IEEE P802.11n Wireless LANS TGn Sync Proposal Technical Specification, August 13, 2004, Compiled by Syed Aol Mujtaba, Agree Systems Inc.

8.1.3 Paper references

[9] G.J. Foschini and M.J. Gans, “On the limits of wireless communications in a fading environment when using multiple antennas”*, Wireless Personal Communications*, vol. 6, March 1998, pp. 311-335.

[10] A.V. Zelst and Tim C.W. Schenk, "Implementation of MIMO OFDM-Based Wireless LAN System" *IEEE Transcations on Signal Processing*, Vol. 52, No.2, February 2004, pp. 483-494

[11] G. J. Foschini, "Layered space-time architecture for wireless communication in a fading environment when using multi-element antennas," Bell Labs Tech. J., pp. 41–59, Autumn 1996.

[12] S.Loyka, F. Gagnon, "Performance Analysis of the V-BLAST Algorithm: An Analytical Approach", *2002 International Zurich Seminar on Broadband Communications*, *Access – Transmission – Networking*.

[13] Amit Gupta, Antonio Forenza and Robert W. Heath Jr.,"Rapid MIMO-OFDM Software Defined Radio System Prototyping" *Proceedings of IEEE Workshop on Signal Processing Systems*.

[14] Antonio Forenza, David J. Love, and Robert W. Heath Jr., "A Low Complexity Algorithm to Simulate the Spatial Covariance Matrix for Clustered MIMO Channel Models" *VTC 2004*.

[15] Helmut Bölcskei, David Gesbert, Arogyaswami J. Paulraj, "On the Capacity of OFDM-Based Spatial Multiplexing Systems", *IEEE TRANSACTIONS ON COMMUNICATIONS*, VOL. 50, NO. 2, FEBRUARY 2002, pp-225 234

[16] Jibing Wang and Kung Yao, "Capacity Scaling in OFDM Based SpatialMultiplexing Systems", Electrical Engineering Department University of California, Los Angeles

[17] Yong Le and Jaekyun Moon, "Performance analysis of Bit-Interleaved Space-Time Coding for OFDM in Block Fading Channels", Department of Electrical and Computer Engineering, University of Minnesota, Minneapolis.

[18] Ben Lu, Xiaodong Wang, Krishna R. Narayanan, "LDPC-Based Space-Time Coded OFDM System Over Correlated Fading Channels: Performance Analysis and Receiver Design", *IEEE*

TRANSACTIONS ON COMMUNICATIONS, VOL 50, NO. 1, JANUARY 2002

[19] S. Alamouti, "A Simple Transmit Diversity Technique for Wireless Communications," *IEEE Journal on Selected Areas in Communications*. vol. 46, pp. 145 l -1458,1998.

[20] Yan Xin and Georgios B. Giannakis "High-Rate Space–Time Layered OFDM", *IEEE COMMUNICATIONS LETTERS*, VOL. 6, NO. 5, MAY 2002

[21] Jooyeol Yang and Kyungwhoon Cheun, "Low Complexity implementation of Alamouti Space-Time Coded OFDM Transmitters", *IEEE COMMUNICATIONS LETTERS*, VOL. 8, NO. 4, APRIL 2004

[22] Ove Edfors et al. "OFDM Channel Estimation by Singular Value Decomposition", *IEEE Transactions on Communications*, vol. 46 no.7, pp. 931-939, July 1998.

[23] P. Khanna, J. Ibrhaim, A. Hebbar et al, "Smart Antenna Applications for WLAN 802.11a" Wireless 2004, Calegery, Cannada